

Sampling Theory for Function Approximation with Numerical Redundancy

Astrid Herremans* and Daan Huybrechs*

Abstract

The study of numerical rounding errors is often greatly simplified in the analytical treatment of mathematical problems, or even entirely separated from it. In sampling theory, for instance, it is standard to assume the availability of an orthonormal basis for computations, ensuring that numerical errors are negligible. In reality, however, this assumption is often unmet. In this paper, we discard it and demonstrate the advantages of integrating numerical insights more deeply into sampling theory. To clearly pinpoint when the numerical phenomena play a significant role, we introduce the concept of *numerical redundancy*. A set of functions is numerically redundant if it spans a lower-dimensional space when analysed numerically rather than analytically. This property makes it generally impossible to compute the best approximation of a function in its span using finite precision. In contrast, ℓ^2 -regularized approximations are computable and, therefore, form the foundation of many practical methods. Regularization generally reduces accuracy compared to the best approximation, but our analysis shows that there is a benefit: it also significantly reduces the amount of data needed for accurate approximation. In this paper, we develop the analytical tools needed to fully understand this effect. Furthermore, we present a constructive method for optimally selecting data points for L^2 -approximations, explicitly accounting for the effects of regularization. The results are illustrated for two common scenarios that lead to numerical redundancy: (1) approximations on irregular domains and (2) approximations that incorporate specific features of the function to be approximated. In doing so, we obtain new results on random sampling for Fourier extension frames. Finally, we establish that regularization is implicit in numerical orthogonalization of a numerically redundant set, indicating that its analysis can not be bypassed in a much broader range of methods.

1 Introduction

We are interested in the problem of computing an approximation to a function f in a Hilbert space H . Due to the focus on computability, this problem will be referred to as numerical approximation. An important aspect is that although the function f generally resides in an infinite-dimensional space, a numerical method can process only a finite number of measurements of f . This naturally leads to the introduction of a sequence of finite-dimensional spaces $\{V_n\}_{n \in \mathbb{N}}$ of increasing dimension n , forming approximations to H . It is hereby assumed, based on prior knowledge, that f is well approximated in the spaces V_n in the sense that fast convergence is attainable. Associated with a numerical approximation is thus an operator $\mathcal{F}_{n,m} : \mathbb{C}^m \rightarrow V_n$ mapping m measurements of a function f to a function $f_{n,m}$ in the approximation space V_n . Note that the number of measurements m can differ from the dimension n . In particular, it is often required that m is sufficiently large compared to n , or equivalently n sufficiently small, in order to obtain robust and accurate approximation methods [3, 18].

Another important aspect of numerical approximation is how to represent an approximation in V_n . The computed approximations $f_{n,m}$ are continuous objects, which cannot be stored directly on a computer. To this end, one needs a spanning set $\Phi_n = \{\phi_{i,n}\}_{i=1}^{n'}$ satisfying $\text{span}(\Phi_n) = V_n$. This allows the approximation $f_{n,m}$ to be characterized by a set of expansion coefficients \mathbf{x}

$$f_{n,m} = \sum_{i=1}^{n'} x_i \phi_{i,n}. \quad (1)$$

*Department of Computer Science, KU Leuven, 3001 Leuven, Belgium (astrid.herremans@kuleuven.be, daan.huybrechs@kuleuven.be)

Note that the spanning set Φ_n does not need to be linearly independent, implying that n' can differ from n , in which case multiple sets of expansion coefficients exist that describe the same function. Associated with a numerical approximation is, therefore, also an operator $\mathcal{L}_{n,m} : \mathbb{C}^m \rightarrow \mathbb{C}^{n'}$ mapping m measurements of a function f to a set of n' expansion coefficients of an approximation $f_{n,m} \in V_n$.

Sampling theory aims to determine the amount of information required from a function f to achieve a (near-)optimal approximation in V_n , while ensuring robustness to noise. Standard results for linear approximation methods are typically obtained by analysing $\mathcal{F}_{n,m}$ and, hence, are independent of the spanning set Φ_n that is used. The underlying assumption is that the numerical computations are performed using an orthonormal or Riesz basis as a spanning set for V_n , such that $\mathcal{L}_{n,m}$ and $\mathcal{F}_{n,m}$ have similar properties. However, this assumption is often not satisfied in practice; many different types of spanning sets show up in a wide variety of applications. Riesz bases for V_n are often unknown and computing them can be numerically unstable. Furthermore, the choice of the spanning set may be influenced by the potential to reduce the computational cost of the method; structured spanning sets can permit the use of fast transforms such as the Fast Fourier Transform.

In particular, many applications make use of a *numerically redundant* spanning set. Such a set might be linearly independent from an analytic point of view, but linearly dependent from a numerical point of view. In this case, regularization is needed to obtain a bounded map $\mathcal{L}_{n,m}$ from measurements to expansion coefficients. In [5, 6], this phenomenon is analysed for regularization by truncation of the singular value decomposition (TSVD). It is shown that the approximation space after regularization is effectively smaller than V_n and, therefore, regularization generally lowers the accuracy. On the other hand, it is also demonstrated that the number of required measurements reduces due to regularization, depending on the spanning set that is used. Hence, in these cases, the choice of the spanning set does influence the sampling theoretical analysis. The primary focus of this paper is identifying when and how the chosen spanning set impacts the required amount of data for accurate function approximation.

We describe the approximation problem in more detail and give known results about sampling for least squares approximations to frame the main contribution and overview of the paper.

1.1 Approximation problem

Let f be a function in a separable Hilbert space H with associated inner product $\langle \cdot, \cdot \rangle_H$ and induced norm $\| \cdot \|_H$. We aim at computing approximations to f in a sequence of finite-dimensional approximation spaces $\{V_n\}_{n \in \mathbb{N}}$ of increasing dimension n , satisfying $V_n \subset H$. We assume that we can process measurements $\mathcal{M}_m f$ ($m = 1, 2, \dots$), where \mathcal{M}_m are linear sampling operators

$$\mathcal{M}_m : G \rightarrow \mathbb{C}^m, \quad f \mapsto \{l_{j,m}(f)\}_{j=1}^m \quad (2)$$

consisting of m functionals $l_{j,m}$, which may depend on m . The operators \mathcal{M}_m may only be defined on a dense subspace $G \subseteq H$ with associated norm $\| \cdot \|_G$, satisfying

$$\|g\|_H^2 \leq C_G \|g\|_G^2, \quad \forall g \in G. \quad (3)$$

We assume that each \mathcal{M}_m is bounded with respect to $\| \cdot \|_G$, i.e.,

$$\|\mathcal{M}_m\|_{G,2} := \sup_{g \in G, g \neq 0} \frac{\|\mathcal{M}_m g\|_2}{\|g\|_G} < \infty,$$

and that $V_n \subset G$ for all $n \in \mathbb{N}$. In what follows, we will also assume that $\|\mathcal{M}_m\|_{G,2} \geq 1$, which can always be achieved via scaling. The operator \mathcal{M}_m defines a semi-norm

$$\| \cdot \|_m := \|\mathcal{M}_m \cdot \|_2. \quad (4)$$

Remark 1. A typical example is the approximation of continuous functions in $H = L^2([-1, 1])$ using pointwise evaluations. In this case, G is the space of continuous functions $C([-1, 1])$ with associated norm $\|g\|_G = \sup_{x \in [-1, 1]} |g(x)|$ satisfying (3) for $C_G = 2$. Furthermore, if

$$\mathcal{M}_m f = \{f(x_{j,m})/\sqrt{m}\}_{j=1}^m$$

for some sample points $x_{j,m} \in [-1, 1]$, then $\|\mathcal{M}_m\|_{G,2} = 1$.

In order to represent the approximations, we use spanning sets $\Phi_n = \{\phi_{i,n}\}_{i=1}^{n'}$ which satisfy $\text{span}(\Phi_n) = V_n$ for all $n \in \mathbb{N}$. The elements $\phi_{i,n}$ may depend on n and characterize the synthesis operator

$$\mathcal{T}_n : \mathbb{C}^{n'} \rightarrow V_n, \quad \mathbf{x} \mapsto \sum_{i=1}^{n'} x_i \phi_{i,n}. \quad (5)$$

Note that n' depends on n yet it is not necessarily equal to n , since Φ_n can in general be linearly dependent. For a certain operator $\mathcal{L}_{n,m} : \mathbb{C}^m \rightarrow \mathbb{C}^{n'}$ from measurements to expansion coefficients, one can now define the approximation $f_{n,m} \in V_n$ as

$$f_{n,m} := \mathcal{T}_n \mathcal{L}_{n,m} (\mathcal{M}_m f + \mathbf{n}) = \mathcal{F}_{n,m} (\mathcal{M}_m f + \mathbf{n}), \quad (6)$$

where

$$\mathcal{F}_{n,m} : \mathbb{C}^m \rightarrow V_n, \quad \mathbf{d} \mapsto \mathcal{T}_n \mathcal{L}_{n,m} \mathbf{d} \quad (7)$$

and $\mathbf{n} \in \mathbb{C}^m$ is measurement noise. The question arises if the approximation is accurate, i.e., if it lies close to the best approximation in V_n and is robust to measurement noise. We will first discuss the well-studied case of least squares approximation.

1.2 Least squares approximation

A typical choice for the map $\mathcal{L}_{n,m}$ is discrete least squares fitting,

$$\mathcal{L}_{n,m}^{\text{LS}} : \mathbb{C}^m \rightarrow \mathbb{C}^{n'}, \quad \mathbf{d} \mapsto \arg \min_{\mathbf{x} \in \mathbb{C}^{n'}} \|\mathcal{M}_m \mathcal{T}_n \mathbf{x} - \mathbf{d}\|_2^2 \quad (8)$$

with associated operator $\mathcal{F}_{n,m}^{\text{LS}}$ defined by (7). The least squares operator $\mathcal{L}_{n,m}^{\text{LS}}$ is linear. For simplicity, we assume that the operator is also uniquely defined, implying that $m \geq n = n'$. The accuracy of a least squares approximation has been studied extensively, see for example [2, 4, 12, 18]. A key ingredient to its analysis is the norm inequality

$$A_{n,m} \|v\|_H^2 \leq \|v\|_m^2, \quad \forall v \in V_n. \quad (9)$$

Similar to [2, Theorem 5.3], the following theorem shows that if the sampling operator satisfies (9) for some $A_{n,m} > 0$, then the error of the discrete least squares approximation is close to optimal and the influence of measurement noise is bounded.

Theorem 1. *If (9) holds for some $A_{n,m} > 0$, then the error of the discrete least squares approximation to $f \in H$ satisfies*

$$\|f - \mathcal{F}_{n,m}^{\text{LS}} \mathbf{f}\|_H \leq \left(\sqrt{C_G} + \frac{\|\mathcal{M}_m\|_{G,2}}{\sqrt{A_{n,m}}} \right) e_n(f) + \frac{1}{\sqrt{A_{n,m}}} \|\mathbf{n}\|_2,$$

where $\mathbf{f} = \mathcal{M}_m f + \mathbf{n} \in \mathbb{C}^m$ is noisy data and

$$e_n(f) := \inf_{v \in V_n} \|f - v\|_G. \quad (10)$$

Proof. If $f \notin G$, then the right-hand side is infinite such that the bound trivially holds. Assuming $f \in G$, one has for any $v \in V_n$

$$\begin{aligned} \|f - \mathcal{F}_{n,m}^{\text{LS}} \mathbf{f}\|_H &\leq \|f - v\|_H + \|v - \mathcal{F}_{n,m}^{\text{LS}} \mathbf{f}\|_H \\ &\leq \|f - v\|_H + \frac{1}{\sqrt{A_{n,m}}} \|v - \mathcal{F}_{n,m}^{\text{LS}} \mathbf{f}\|_m && \text{(using (9))} \\ &\leq \|f - v\|_H + \frac{1}{\sqrt{A_{n,m}}} \|\mathcal{M}_m v - \mathbf{f}\|_2 \\ &\leq \|f - v\|_H + \frac{1}{\sqrt{A_{n,m}}} (\|v - f\|_m + \|\mathbf{n}\|_2) \\ &\leq \left(\sqrt{C_G} + \frac{\|\mathcal{M}_m\|_{G,2}}{\sqrt{A_{n,m}}} \right) \|f - v\|_G + \frac{1}{\sqrt{A_{n,m}}} \|\mathbf{n}\|_2 && \text{(boundedness of } \mathcal{M}_m \text{ and (3))} \end{aligned}$$

where in the third step we used that $\mathcal{M}_m \mathcal{F}_{n,m}^{\text{LS}}$ is a projection onto $\{\mathcal{M}_m v \mid v \in V_n\}$ such that

$$\|\mathcal{M}_m v - \mathcal{M}_m \mathcal{F}_{n,m}^{\text{LS}} \mathbf{f}\|_2 = \|\mathcal{M}_m \mathcal{F}_{n,m}^{\text{LS}} \mathcal{M}_m v - \mathcal{M}_m \mathcal{F}_{n,m}^{\text{LS}} \mathbf{f}\|_2 \leq \|\mathcal{M}_m v - \mathbf{f}\|_2.$$

□

Remark 2. *In this paper, we limit ourselves to error bounds that depend on the optimal error measured in the G -norm. Deriving bounds in terms of the H -norm is typically more challenging. For instance, probabilistic error bounds of this kind can be obtained when considering random pointwise samples for $H = L^2$ approximations, as demonstrated in [19, 23].*

Assume that we can identify a function $\gamma : \mathbb{N} \rightarrow \mathbb{N}$ such that there exists a constant A satisfying $0 < A \leq A_{n,\gamma(n)}$ for all $n \in \mathbb{N}$. Then, the operators $\mathcal{F}_{n,\gamma(n)}^{\text{LS}}$ have near-optimal accuracy and are robust to noise as described by Theorem 1, for all $n \in \mathbb{N}$. In this case, A is referred to as the lower bound of a Marcinkiewicz-Zygmund inequality for the doubly-indexed set of sampling functionals $\{l_{j,\gamma(n)} : n \in \mathbb{N}, j = 1 \dots \gamma(n)\}$ [29].

It follows from Theorem 1 that the accuracy and robustness of least squares approximations depend solely on $A_{n,m}$, C_G and $\|\mathcal{M}_m\|_{G,2}$, which in turn do not depend on the chosen spanning set Φ_n . However, recall from (6) that one cannot directly compute $\mathcal{F}_{n,m}^{\text{LS}}$, yet computes expansion coefficients via $\mathcal{L}_{n,m}^{\text{LS}}$. Hence, the numerical stability of the algorithm also depends on $\mathcal{L}_{n,m}^{\text{LS}}$, which can behave wildly for certain choices of Φ_n . More specifically, it holds for any $\mathbf{d} \in \mathbb{C}^m$ that

$$\mathcal{L}_{n,m}^{\text{LS}} \mathbf{d} = (\mathcal{M}_m \mathcal{T}_n)^\dagger \mathbf{d}, \quad (11)$$

where † denotes the Moore-Penrose pseudo-inverse. Therefore,

$$\|\mathcal{L}_{n,m}^{\text{LS}}\|_{2,2} = \frac{1}{\sigma_{\min}(\mathcal{M}_m \mathcal{T}_n)} \geq \frac{1}{K \sigma_{\min}(\mathcal{T}_n)},$$

where $\sigma_{\min}(\cdot)$ denotes the smallest nonzero singular value and $K := \max_{v \in V_n, \|v\|_H=1} \|v\|_m$. As explained in section 2, $\sigma_{\min}(\mathcal{T}_n)$ is close to zero for numerically redundant spanning sets and, hence, regularization is generally needed to obtain a bounded operator $\mathcal{L}_{n,m}$ mapping measurements to expansion coefficients. The goal of this paper is to deepen our understanding of sampling for numerically redundant spanning sets Φ_n , taking into account the effects of regularization.

1.3 Main contribution

As mentioned in the introduction, the influence of ℓ^2 -regularization in the case of a numerically redundant spanning set was first highlighted in [5, 6]. This led to an analysis of the truncated singular value decomposition (TSVD) as a means for regularizing least squares approximations. The accuracy of a TSVD approximation is described in [6, Theorem 1.3] and depends on a regularization parameter, as well as on the existence of accurate approximations with small expansion coefficients. Furthermore, the accuracy depends on two constants, $\kappa_{M,N}^\epsilon$ and $\lambda_{M,N}^\epsilon$, which characterize the influence of discretization. These constants are influenced by regularization, yet in a non-transparent way.

The primary goal of this paper is to deepen our understanding of sampling for ℓ^2 -regularized least squares approximations. Our main contribution is the identification of a new norm inequality, analogous to that of unregularized least squares approximation (9), which fully characterizes the accuracy and conditioning of these methods. The following results are part of Theorem 7 and 8.

Theorem 2. *Consider the ℓ^2 -regularized least squares operator*

$$\mathcal{L}_{n,m}^{\text{RLS}} : \mathbb{C}^m \rightarrow \mathbb{C}^{n'}, \quad \mathbf{d} \mapsto \arg \min_{\mathbf{x} \in \mathbb{C}^{n'}} \|\mathbf{d} - \mathcal{M}_m \mathcal{T}_n \mathbf{x}\|_2^2 + \epsilon^2 \|\mathbf{x}\|_2^2, \quad (12)$$

with associated operator $\mathcal{F}_{n,m}^{\text{RLS}}$ defined by (7). If

$$A_{n,m}^\epsilon \|\mathcal{T}_n \mathbf{x}\|_H^2 \leq \|\mathcal{T}_n \mathbf{x}\|_m^2 + \epsilon^2 \|\mathbf{x}\|_2^2, \quad \forall \mathbf{x} \in \mathbb{C}^{n'}, \quad (13)$$

holds for some $A_{n,m}^\epsilon > 0$, then the error of the discrete regularized least squares approximation to $f \in H$ satisfies

$$\|f - \mathcal{F}_{n,m}^{\text{RLS}} \mathbf{f}\|_H \leq \left(\sqrt{C_G} + \frac{(1 + \sqrt{2}) \|\mathcal{M}_m\|_{G,2}}{\sqrt{A_{n,m}^\epsilon}} \right) e_n^\epsilon(f) + \frac{1 + \sqrt{2}}{\sqrt{A_{n,m}^\epsilon}} \|\mathbf{n}\|_2,$$

where $\mathbf{f} = \mathcal{M}_m f + \mathbf{n} \in \mathbb{C}^m$ is noisy data and

$$e_n^\epsilon(f) := \inf_{\mathbf{x} \in \mathbb{C}^{n'}} \|f - \mathcal{T}_n \mathbf{x}\|_G + \epsilon \|\mathbf{x}\|_2. \quad (14)$$

Furthermore, the absolute condition number of $\mathcal{F}_{n,m}^{RLS}$ can be bounded by

$$\kappa_{n,m}^{RLS} \leq \frac{1 + \sqrt{2}}{\sqrt{A_{n,m}^\epsilon}}. \quad (15)$$

Remark 3. Here, $\epsilon > 0$ is a regularization parameter that is of the order of ϵ_{mach} , the working precision associated with the numerical computations, as discussed in section 2.3. This unorthodox choice of symbol for the regularization parameter emphasizes that it is small and that regularization is purely due to a finite working precision.

A couple of important conclusions are in order. First and foremost, (13) is a relaxation of (9); one can always find $A_{n,m}^\epsilon \geq A_{n,m}$. In order to see why, observe that both norm inequalities are equivalent for $\epsilon = 0$, i.e., in the case of working with infinite precision. In other words: it is easier to satisfy (13) than (9) and, hence, regularization can only reduce the required amount of data. After formally introducing the concept of numerical redundancy, it will become clear that this relaxation is significant only for numerically redundant spanning sets. Second, the accuracy is now governed by (14) as opposed to (10). As discussed in section 2.2, this behaviour is expected when approximating with finite precision. As a result, the size of the expansion coefficients $\|\mathbf{x}\|_2$ is an important object of study, which was also one of the main conclusions of [5, 6]. Third, whereas (9) solely depends on the sampling operator \mathcal{M}_m and the approximation space V_n , (13) also depends on the spanning set Φ_n and the regularization parameter ϵ . These additional dependencies make its analysis significantly more complicated.

These results offer a new perspective on the influence of finite precision. While finite precision requires regularization, which generally reduces accuracy compared to the best approximation, there is a benefit: regularization also decreases the amount of required information. Predicting the exact interplay between these two effects is, however, challenging. The main difficulty lies in the dependency of (13) and (14) on the specific spanning set Φ_n . Whereas earlier work has focused on the influence of regularization on the convergence behaviour [5, 6], we develop the tools to understand its influence on the associated sampling problem.

1.4 Paper Overview

In section 2, we formalize the notion of numerical redundancy using ideas from low rank matrix theory and harmonic analysis. Our primary goal is to clearly identify when the effects discussed in this paper are significant. Using this framework we prove that the achievable error of a numerical approximation deviates from the analytical best approximation error, particularly if the spanning set is numerically redundant. Furthermore, through a backward stability analysis we show that simple least squares fitting generally fails to produce accurate results in the presence of numerical redundancy, while the accuracy of ℓ^2 -regularized approximations is close to optimal from a numerical point of view. The results in section 2 also hint at the idea that the effects of finite precision cannot be overcome through straightforward numerical orthogonalization. This is investigated further in section 6, where it is demonstrated that regularization is implicit in numerical orthogonalization of a numerically redundant set. This implies that the results of this paper are relevant for a much broader class of methods.

Due to the necessity of ℓ^2 -regularization when computing with numerically redundant spanning sets, it is worthwhile to take regularization into account during discretization. Section 3 formalizes how regularization relaxes the discretization condition, resulting in a decrease of the amount of data required for accurate function approximation. Our analysis is not limited to TSVD regularization, or even ℓ^2 -regularization; instead, we present a unified framework for regularized least squares problems with a general penalty term as the underlying methodology seamlessly extends. In section 4, we show an additional advantage of the formulation (13): it enables constructive methods for selecting the sampling functionals $l_{j,m}$. Specifically, we identify an efficient random sampling distribution for L^2 -approximations that takes into account the influence of regularization. Section 5 applies the results to two settings of numerically redundant approximations: approximation that incorporates prior

knowledge about the asymptotic behaviour of the function to be approximated and approximation on irregular domains. In doing so, we obtain new results on sampling for Fourier extension frames. Specifically, we show that only a log-linear amount of uniformly random samples is sufficient for convergence down to machine precision in a Fourier extension frame. In contrast, an analysis that ignores the effects of regularization would suggest a need for quadratic oversampling.

2 Approximating with finite precision

In this section, we discuss the influence of working with a finite relative precision, yet we do so before introducing a discretization for the problem at hand. An advantage of this approach is that the results do not depend on the properties of a sampling operator. However, this also means that whereas we gain insight in numerical approximation, the results in this section are not yet numerically computable.

2.1 Numerical redundancy

Consider a spanning set $\Phi_n = \{\phi_{i,n}\}_{i=1}^{n'}$ for the approximation space V_n of dimension n , i.e., Φ_n satisfies $\text{span}(\Phi_n) = V_n$. Analytically, Φ_n is linearly dependent only when $n' > n$. In this case, there exists a nonzero coefficient vector $\mathbf{x} \in \mathbb{C}^{n'}$ that satisfies

$$\sum_{i=1}^{n'} x_i \phi_{i,n} = \mathcal{T}_n \mathbf{x} = 0,$$

i.e., \mathbf{x} lies in the kernel of the synthesis operator \mathcal{T}_n (5). When computing numerically, the notion of linear dependency changes drastically since computations can only be performed with a finite working precision ϵ_{mach} . On a machine with finite precision, a vector \mathbf{x} is stored as $\bar{\mathbf{x}}$ where

$$\bar{\mathbf{x}} = \mathbf{x} + \Delta \mathbf{x} \quad \text{with} \quad \|\Delta \mathbf{x}\|_2 \leq \epsilon_{\text{mach}} \|\mathbf{x}\|_2.$$

This error propagates through the calculations

$$\|\mathcal{T}_n \bar{\mathbf{x}} - \mathcal{T}_n \mathbf{x}\|_2 = \|\mathcal{T}_n \Delta \mathbf{x}\|_2 \leq \epsilon_{\text{mach}} \|\mathcal{T}_n\|_{2,H} \|\mathbf{x}\|_2. \quad (16)$$

It follows from this simple error analysis that a nonzero vector \mathbf{x} might lie in the kernel of \mathcal{T}_n if calculations show that $\|\mathcal{T}_n \bar{\mathbf{x}}\|_2 \leq \epsilon_{\text{mach}} \|\mathcal{T}_n\|_{2,H} \|\mathbf{x}\|_2$.

To take into account the influence of finite precision, it is customary in low rank matrix theory to introduce a numerical rank. Whereas the rank of \mathcal{T}_n equals n , its ϵ -rank can be defined analogously to [28] by

$$r = \inf\{\text{rank}(\mathcal{X}_n) : \|\mathcal{T}_n - \mathcal{X}_n\|_{2,H} \leq \epsilon \|\mathcal{T}_n\|_{2,H}\}, \quad (17)$$

where the infimum is taken over all linear operators \mathcal{X}_n mapping from $\mathbb{C}^{n'}$ to H . The ϵ -rank takes into account that, in the presence of rounding errors, the computed output $\mathcal{T}_n \bar{\mathbf{x}}$ behaves similarly as the exact output $\mathcal{X}_n \mathbf{x}$ of some linear operator \mathcal{X}_n that lies close to \mathcal{T}_n . Indeed, similarly to (16) one has

$$\|\mathcal{X}_n \mathbf{x} - \mathcal{T}_n \mathbf{x}\|_2 \leq \epsilon \|\mathcal{T}_n\|_{2,H} \|\mathbf{x}\|_2$$

for all \mathcal{X}_n satisfying $\|\mathcal{T}_n - \mathcal{X}_n\|_{2,H} \leq \epsilon \|\mathcal{T}_n\|_{2,H}$. If $r < n$ for $\epsilon = \epsilon_{\text{mach}}$, the operator \mathcal{T}_n is numerically rank-deficient, meaning that it is within the relative tolerance ϵ_{mach} of an operator with rank less than n . In this case, we say that Φ_n is numerically redundant.

Definition 1. A spanning set Φ_n for the n -dimensional space V_n is called “numerically redundant” if the ϵ -rank of its synthesis operator \mathcal{T}_n is strictly less than n , where $\epsilon = \epsilon_{\text{mach}}$ is the working precision associated with the numerical computations.

An elegant characterization of numerically redundant spanning sets follows from the field of harmonic analysis. To this end we introduce frames, which extend the concept of a Riesz basis to allow for the inclusion of linearly dependent sets. As defined by [17, Definition 1.1.1], the set Φ_n is a frame for V_n if there exist frame bounds $0 < A_n \leq B_n$ such that

$$A_n \|f\|_H^2 \leq \sum_{i=1}^{n'} |\langle f, \phi_{i,n} \rangle_H|^2 \leq B_n \|f\|_H^2, \quad \forall f \in V_n. \quad (18)$$

If we refer to the frame bounds A_n and B_n of Φ_n we will always assume that they are optimal, meaning that they are the largest and smallest constant that satisfy (18), respectively. A_n and B_n always exist, since every finite set is a frame for its span [17, Corollary 1.1.3]. Furthermore, they satisfy

$$A_n = \sigma_{\min}(\mathcal{T}_n)^2 \quad \text{and} \quad B_n = \sigma_{\max}(\mathcal{T}_n)^2 \quad [17, \text{Theorem 1.3.1}], \quad (19)$$

where σ_{\min} and σ_{\max} denote the smallest and largest nonzero singular values.

From here, it follows that the lower frame bound is intrinsically linked to the size of the expansion coefficients. Namely, for any function $f \in V_n$, there exist expansion coefficients $\mathbf{x} \in \mathbb{C}^{n'}$ that satisfy

$$f = \mathcal{T}_n \mathbf{x} \quad \text{and} \quad \|\mathbf{x}\|_2 \leq \|f\|_H / \sqrt{A_n}. \quad (20)$$

If the frame is linearly dependent, an infinite number of other sets of expansion coefficients describing the same function exist as well. If the lower frame bound lies close to zero no expansion can be found with reasonably sized coefficients, at least for some functions in V_n . This is precisely what happens in the case of a numerically redundant spanning set, as demonstrated by the following property.

Property 1. *A spanning set Φ_n is numerically redundant if and only if its frame bounds defined by (18) satisfy*

$$A_n \leq \epsilon_{\text{mach}}^2 B_n.$$

Proof. From the extremal properties of singular values [13, Lecture 23], it follows that

$$\min_{\text{rank}(\mathcal{X}_n) < n} \|\mathcal{T}_n - \mathcal{X}_n\|_{2,H} = \sigma_{\min}(\mathcal{T}_n),$$

where the minimum is taken over all linear operators \mathcal{X}_n mapping from $\mathbb{C}^{n'}$ to H . Combining this result with Definition 1, one can conclude the Φ_n is numerically redundant if and only if the smallest nonzero singular value of \mathcal{T}_n is less than or equal to $\epsilon_{\text{mach}} \|\mathcal{T}_n\|_{2,H}$. The final result follows (19). \square

In many applications, consecutive spanning sets $\Phi_n = \{\phi_{i,n}\}_{i=1}^{n'}$ for the approximation spaces $\{V_n\}_{n \in \mathbb{N}}$ are finite subsequences of an infinite set $\Psi = \{\psi_i\}_{i=1}^{\infty}$, satisfying $\text{span}(\Psi) = H$. More specifically, one chooses

$$\phi_{i,n} = \psi_i, \quad 1 \leq i \leq n', \quad \forall n \in \mathbb{N}. \quad (21)$$

Based on the properties of Ψ , one can determine whether Φ_n is numerically redundant for sufficiently large n . In [5, section 4] this is analysed for a linearly independent infinite-dimensional frame Ψ . A set Ψ is an infinite-dimensional frame for H if there exist constants $A, B > 0$ such that

$$A \|f\|_H^2 \leq \sum_{i=1}^{\infty} |\langle f, \psi_i \rangle_H|^2 \leq B \|f\|_H^2, \quad \forall f \in H. \quad (22)$$

Furthermore, Ψ is linearly independent if every finite subsequence is linearly independent [17, §3-4]. Note that in contrast to the finite-dimensional case, it does not hold that every infinite set is a frame for its closed span. Again, if we refer to the frame bounds A and B of Ψ we assume that they are optimal. If Ψ is a frame for H , analogously to (20) one has that for any $f \in H$ there exist coefficients $\mathbf{x} \in \ell^2(\mathbb{N})$ satisfying

$$f = \sum_{i=1}^{\infty} \psi_i x_i \quad \text{and} \quad \|\mathbf{x}\|_2 \leq \|f\|_H / \sqrt{A}, \quad [17, \text{Lemma 5.5.5}]. \quad (23)$$

Assuming that Ψ is a linearly independent frame, numerical redundancy can now be identified from analysing the upper and lower frame bound of Φ_n as n increases. Following [5, Lemma 5], the upper frame bound B_n behaves nicely; it is shown that $\{B_n\}_{n \in \mathbb{N}}$ is monotonically increasing and $B_n \rightarrow B$, as $n \rightarrow \infty$. However, the lower frame bound A_n can behave wildly; it is shown that $\{A_n\}_{n \in \mathbb{N}}$ is monotonically decreasing and $\inf_n A_n = 0$ if Ψ is overcomplete, which means that there exist unit-norm coefficients $\mathbf{c} \in \ell^2(\mathbb{N})$ for which

$$\sum_{i=1}^{\infty} \psi_i c_i = 0.$$

We can conclude that if Ψ is an overcomplete frame, the lower frame bound A_n of the subsequence Φ_n will inevitably drop below $\epsilon_{\text{mach}}^2 \|\mathcal{T}_n\|_{2,H} = \epsilon_{\text{mach}}^2 B_n^2$ for sufficiently large n , resulting in a numerically redundant spanning set Φ_n according to Property 1. This is not the case for subsequences of Riesz bases [17, Theorem 3.6.6 (ii)].

2.2 Achievable accuracy of numerical approximations

As motivated in the previous section, when one computes the output of the operator \mathcal{T}_n using a finite working precision ϵ_{mach} , the result can be modeled as the output of some other linear operator \mathcal{X}_n that also maps from $\mathbb{C}^{n'}$ to H and that lies close to \mathcal{T}_n

$$\|\mathcal{T}_n - \mathcal{X}_n\|_{2,H} \leq \epsilon_{\text{mach}} \|\mathcal{T}_n\|_{2,H}. \quad (24)$$

The range of \mathcal{X}_n , denoted by $\text{R}(\mathcal{X}_n)$, is generally not equal to V_n . Hence, the approximation space changes. To analyse this effect, we examine the error of the best approximation to a function $f \in H$, i.e., its orthogonal projection onto $\text{R}(\mathcal{X}_n)$.

Theorem 3. *For any $f \in H$, the error of the orthogonal projection onto the range of a linear operator $\mathcal{X}_n : \mathbb{C}^{n'} \rightarrow H$ that satisfies (24) is bounded by*

$$\|f - \widehat{P}_n f\|_H \leq \|f - \mathcal{T}_n \mathbf{x}\|_H + \epsilon_{\text{mach}} \|\mathcal{T}_n\|_{2,H} \|\mathbf{x}\|_2, \quad \forall \mathbf{x} \in \mathbb{C}^{n'},$$

where \widehat{P}_n denotes the orthogonal projector onto $\text{R}(\mathcal{X}_n)$. Furthermore, using the frame bounds of Φ_n introduced in (18), this implies

$$\|f - \widehat{P}_n f\|_H \leq \|f - P_n f\|_H + \epsilon_{\text{mach}} \sqrt{\frac{B_n}{A_n}} \|f\|_H,$$

where P_n denotes the orthogonal projector onto the approximation space $V_n = \text{R}(\mathcal{T}_n)$.

Proof. Using $f = (f - \mathcal{T}_n \mathbf{x}) + \mathcal{T}_n \mathbf{x}$, $\forall \mathbf{x} \in \mathbb{C}^{n'}$, it follows that

$$\begin{aligned} \|f - \widehat{P}_n f\|_H &= \|(I - \widehat{P}_n)f\|_H \\ &= \|(I - \widehat{P}_n)((f - \mathcal{T}_n \mathbf{x}) + \mathcal{T}_n \mathbf{x})\|_H \\ &\leq \|I - \widehat{P}_n\|_{H,H} \|f - \mathcal{T}_n \mathbf{x}\|_H + \|(I - \widehat{P}_n)\mathcal{T}_n\|_{2,H} \|\mathbf{x}\|_2, \end{aligned}$$

where $I : H \rightarrow H$ denotes the identity operator. The final result follows from the fact that $I - \widehat{P}_n$ is a projector having unit operator norm, and

$$\|(I - \widehat{P}_n)\mathcal{T}_n\|_{2,H} \leq \|(I - \widehat{P}_n)\mathcal{X}_n\|_{2,H} + \|I - \widehat{P}_n\|_{H,H} \|\mathcal{T}_n - \mathcal{X}_n\|_{2,H} \leq \epsilon_{\text{mach}} \|\mathcal{T}_n\|_{2,H}.$$

The second result follows from the fact that $P_n f \in V_n$ and, therefore, there exist coefficients $\mathbf{c} \in \mathbb{C}^{n'}$ such that $P_n f = \mathcal{T}_n \mathbf{c}$ with $\|\mathbf{c}\|_2 \leq \|P_n f\|_H / \sqrt{A_n}$ (20). Hence, choosing $\mathbf{x} = \mathbf{c}$ and using (19), it follows that

$$\|f - \widehat{P}_n f\|_H \leq \|f - \mathcal{T}_n \mathbf{c}\|_H + \epsilon_{\text{mach}} \sqrt{B_n} \|\mathbf{c}\|_2 \leq \|f - P_n f\|_H + \epsilon_{\text{mach}} \sqrt{\frac{B_n}{A_n}} \|P_n f\|_H.$$

The final result follows from $\|P_n f\|_H \leq \|f\|_H$. \square

Theorem 3 shows that one is guaranteed that accurate approximations are computable with finite precision, if an approximation in V_n exists that is both accurate and can be expanded in Φ_n with reasonably sized coefficients \mathbf{x} . Furthermore, it shows that the analytical best approximation is computable up to an error of order ϵ_{mach} if the frame bounds of Φ_n satisfy $A_n \approx B_n$. On the other hand, for numerically redundant Φ_n , we have $\sqrt{B_n/A_n} \geq 1/\epsilon_{\text{mach}}$ implying that accuracy cannot be guaranteed. In this case, the accuracy of the numerical approximation is generally significantly lower than the analytical best approximation in V_n .

Analogous to section 2.1, one can analyse what happens as $n \rightarrow \infty$ if the spanning sets Φ_n for the approximation spaces $\{V_n\}_{n \in \mathbb{N}}$ are subsequences of an infinite-dimensional set $\Psi = \{\psi_i\}_{i=1}^{\infty}$ as defined by (21). As previously discussed, if Ψ is an overcomplete frame, the finite spanning sets Φ_n are numerically redundant as $n \rightarrow \infty$. According to Theorem 3, this means that high accuracy is not guaranteed for fixed n . However, the following theorem shows that convergence down to ϵ_{mach} is guaranteed as $n \rightarrow \infty$. This is related to the existence of accurate approximations with reasonably sized expansion coefficients as $n \rightarrow \infty$.

Theorem 4. Suppose $\{\Phi_n\}_{n \in \mathbb{N}}$ are defined by (21), Ψ satisfies (22) for some $A, B > 0$ and $\{\mathcal{X}_n\}_{n \in \mathbb{N}}$ is a sequence of linear operators mapping from $\mathbb{C}^{n'}$ to H while satisfying (24) for each $n \in \mathbb{N}$. Then, for any $f \in H$,

$$\lim_{n \rightarrow \infty} \|f - \widehat{P}_n f\|_H \leq \epsilon_{\text{mach}} \sqrt{\frac{B}{A}} \|f\|_H,$$

where \widehat{P}_n denotes the orthogonal projector onto $\text{R}(\mathcal{X}_n)$.

Proof. Using Theorem 3, (21) and $\lim_{n \rightarrow \infty} \|\mathcal{T}_n\|_{2,H} = \lim_{n \rightarrow \infty} \sqrt{B_n} = \sqrt{B}$ [5, Lemma 5], we find that

$$\begin{aligned} \|f - \widehat{P}_n f\|_H &\leq \|f - \mathcal{T}_n \mathbf{x}\|_H + \epsilon_{\text{mach}} \|\mathcal{T}_n\|_{2,H} \|\mathbf{x}\|_2, & \forall \mathbf{x} \in \mathbb{C}^{n'}, \\ \lim_{n \rightarrow \infty} \|f - \widehat{P}_n f\|_H &\leq \left\| f - \sum_{i=1}^{\infty} \psi_i x_i \right\|_H + \epsilon_{\text{mach}} \sqrt{B} \|\mathbf{x}\|_2, & \forall \mathbf{x} \in \ell^2(\mathbb{N}). \end{aligned}$$

Note that the infinite sum $\sum_{i=1}^{\infty} \psi_i x_i$ converges for all $\mathbf{x} \in \ell^2(\mathbb{N})$ since Ψ is a Bessel sequence [17, Theorem 3.2.3]. Furthermore, it follows from (23) that there exist coefficients $\mathbf{c} \in \ell^2(\mathbb{N})$ satisfying $f = \sum_{i=1}^{\infty} \psi_i c_i$ with $\|\mathbf{c}\|_2 \leq \|f\|_H / \sqrt{A}$. Hence, choosing $\mathbf{x} = \mathbf{c}$,

$$\lim_{n \rightarrow \infty} \|f - \widehat{P}_n f\| \leq \left\| f - \sum_{i=1}^{\infty} \psi_i c_i \right\| + \epsilon_{\text{mach}} \sqrt{B} \|\mathbf{c}\|_2 \leq \epsilon_{\text{mach}} \sqrt{\frac{B}{A}} \|f\|_H.$$

□

2.3 Backward stability and the need for ℓ^2 -regularization

In the previous sections, we introduced numerical redundancy and showed that rounding errors effectively change the approximation space. In this section, we analyse how to actually retrieve approximations, assuming we can make use of backward stable algorithms. In this setting, we will come to a similar yet stronger conclusion: accuracy is only guaranteed if the algorithm outputs expansion coefficients with reasonably sized coefficients. This naturally leads to an interest in ℓ^2 -regularized approximations. As mentioned in the introduction of this section, in a more practical setting this analysis would be performed after discretization.

The assumption of backward stability is common in the field of numerical analysis. It is mentioned in [34, section 1.5] that a method for computing $y = f(x)$ is called backward stable if, for any x , it produces a computed \widehat{y} with a small backward error, that is, $\widehat{y} = f(x + \Delta x)$ for some small Δx . In what follows, we assume that *small* means that the perturbations can be bounded by $\|\Delta x_i\| \leq C \epsilon_{\text{mach}} \|x_i\|$ for all inputs x_i , with $C > 0$ a modest constant which may depend on the dimensions of $\{x_i\}_i$. In this case, we say that the algorithm is backward stable with stability constant C . Importantly, the perturbation Δx does not only stem from rounding of the input x , but it also models the effect of rounding errors appearing throughout the calculation of $f(x)$.

First, we analyse the problem of computing the expansion coefficients of the orthogonal projection of a function f onto V_n , i.e.,

$$(f, \mathcal{T}_n) \mapsto \mathbf{c} = \mathcal{T}_n^\dagger f \in \arg \min_{\mathbf{x} \in \mathbb{C}^{n'}} \|f - \mathcal{T}_n \mathbf{x}\|_H^2. \quad (25)$$

Note that if Φ_n is linearly dependent, an infinite number of other sets of expansion coefficients exist for the orthogonal projection, yet the coefficients returned by (25) have the smallest ℓ^2 -norm. The following theorem shows that backward stability does not necessarily guarantee high accuracy for all $f \in H$ if Φ_n is numerically redundant. Its proof can be found in Appendix A.

Theorem 5. Given a function $f \in H$ and coefficients $\widehat{\mathbf{c}}$ computed by a backward stable algorithm for (25) with stability constant C . Then,

$$\|f - \mathcal{T}_n \widehat{\mathbf{c}}\|_H \leq \|f - \mathcal{T}_n \mathbf{x}\|_H + C \epsilon_{\text{mach}} (\|\mathcal{T}_n\|_{2,H} (\|\widehat{\mathbf{c}}\|_2 + \|\mathbf{x}\|_2) + 2\|f\|_H), \quad \forall \mathbf{x} \in \mathbb{C}^{n'}.$$

Furthermore, if Φ_n is linearly independent and satisfies (18) for some $A_n > C^2 \epsilon_{\text{mach}}^2 B_n$, then this implies

$$\|f - \mathcal{T}_n \widehat{\mathbf{c}}\|_H \leq \|f - P_{V_n} f\|_H + C \epsilon_{\text{mach}} \left(\frac{(1 + C \epsilon_{\text{mach}}) \sqrt{B_n}}{\sqrt{A_n} - C \epsilon_{\text{mach}} \sqrt{B_n}} + \sqrt{\frac{B_n}{A_n}} + 2 \right) \|f\|_H.$$

The previous theorem shows that backward stable algorithms for (25) give accurate results if Φ has a sufficiently large lower frame bound A_n . However, for numerically redundant spanning sets, no guarantees can be made. The error can be large, since $\hat{\mathbf{c}}$ can grow unacceptably as A_n goes to zero. Therefore, it is natural to force the solution to have a bounded ℓ^2 -norm by computing a regularized approximation instead

$$(f, \mathcal{T}_n) \mapsto \mathbf{c} = \arg \min_{\mathbf{x} \in \mathbb{C}^{n'}} \|f - \mathcal{T}_n \mathbf{x}\|_H^2 + \epsilon^2 \|\mathbf{x}\|_2^2, \quad (26)$$

where $\epsilon > 0$ is a regularization parameter. Note that this mapping is again linear and that \mathbf{c} is uniquely determined even if the spanning set Φ_n is linearly dependent. The following theorem shows that for sufficiently large ϵ , backward stability does guarantee an error that is close to the achievable accuracy for numerical approximations, as identified in Theorem 3. The proof of Theorem 6 can be found in Appendix A.

Theorem 6. *Given a function $f \in H$ and coefficients $\hat{\mathbf{c}}$ computed by a backward stable algorithm for (26) with stability constant C . If $\epsilon \geq C \epsilon_{mach} \|\mathcal{T}_n\|_{2,H}$, then*

$$\|f - \mathcal{T}_n \hat{\mathbf{c}}\|_H \leq \sqrt{2} \|f - \mathcal{T}_n \mathbf{x}\|_H + (1 + \sqrt{2}) \epsilon \|\mathbf{x}\|_2 + (1 + \sqrt{2}) C \epsilon_{mach} \|f\|_H, \quad \forall \mathbf{x} \in \mathbb{C}^{n'}.$$

3 Discrete regularized least squares approximations

The close relationship between numerically redundant spanning sets and ℓ^2 -regularization motivates the study of discrete regularized least squares approximations, which is detailed in this section. We begin by analysing regularized least squares approximations with a more general penalty term, as the methodology we use naturally extends to such a setting. In section 3.2, we discuss ℓ^2 -regularization, particularly for function approximation with a numerically redundant spanning set.

3.1 Regularized approximation with a general penalty term

Consider the following regularized least squares operator

$$\mathcal{L}_{n,m}^{\text{RLS}} : \mathbb{C}^m \rightarrow \mathbb{C}^{n'}, \quad \mathbf{d} \mapsto \arg \min_{\mathbf{x} \in \mathbb{C}^{n'}} \|\mathbf{d} - \mathcal{M}_m \mathcal{T}_n \mathbf{x}\|_2^2 + p_\epsilon(\mathbf{x}), \quad (27)$$

with associated operator $\mathcal{F}_{n,m}^{\text{RLS}}$ defined by (7). We assume that $\mathcal{L}_{n,m}^{\text{RLS}}$ is well defined, i.e., that the minimizer is unique. The penalty function $p_\epsilon : \mathbb{C}^{n'} \rightarrow \mathbb{R}^+$ can depend on a regularization parameter ϵ . Furthermore, we assume that p_ϵ is even and that $\sqrt{p_\epsilon}$ is subadditive, meaning that for all $\mathbf{x}, \mathbf{y} \in \mathbb{C}^{n'}$ it holds that

$$\sqrt{p_\epsilon(\mathbf{x} + \mathbf{y})} \leq \sqrt{p_\epsilon(\mathbf{x})} + \sqrt{p_\epsilon(\mathbf{y})}. \quad (28)$$

Note that for any subadditive penalty term p_ϵ (28) is automatically satisfied. Typical examples of penalty functions are related to (semi-)norms.

Section 1.2 shows that the accuracy of discrete least squares approximations depends on the norm inequality (9). The following theorem shows that the accuracy of regularized least squares approximations is dictated by a similar norm inequality

$$A_{n,m}^\epsilon \|\mathcal{T}_n \mathbf{x}\|_H^2 \leq \|\mathcal{T}_n \mathbf{x}\|_m^2 + p_\epsilon(\mathbf{x}), \quad \forall \mathbf{x} \in \mathbb{C}^{n'}. \quad (29)$$

Observe that the two inequalities are identical if $p_\epsilon(\mathbf{x}) = 0, \forall \mathbf{x} \in \mathbb{C}^{n'}$. Furthermore, (29) can be viewed as a relaxation of (9), because if (9) holds for some $A_{n,m} > 0$ then (29) automatically holds for $A_{n,m}^\epsilon = A_{n,m}$ (using the assumption that p_ϵ is nonnegative). Analogously to Theorem 1, if the sampling operator satisfies (29) for some $A_{n,m}^\epsilon > 0$, then the error of the discrete regularized least squares approximation is close to optimal and the influence of measurement noise is bounded.

Theorem 7. *If (29) holds for some $A_{n,m}^\epsilon > 0$, then the error of the discrete regularized least squares approximation (27) to $f \in H$ satisfies*

$$\|f - \mathcal{F}_{n,m}^{\text{RLS}} \mathbf{f}\|_H \leq \left(\sqrt{C_G} + \frac{(1 + \sqrt{2}) \|\mathcal{M}_m\|_{G,2}}{\sqrt{A_{n,m}^\epsilon}} \right) e_n^\epsilon(f) + \frac{1 + \sqrt{2}}{\sqrt{A_{n,m}^\epsilon}} \|\mathbf{n}\|_2,$$

where $\mathbf{f} = \mathcal{M}_m f + \mathbf{n} \in \mathbb{C}^m$ is noisy data and

$$e_n^\epsilon(f) := \inf_{\mathbf{x} \in \mathbb{C}^{n'}} \|f - \mathcal{T}_n \mathbf{x}\|_G + \sqrt{p_\epsilon(\mathbf{x})}. \quad (30)$$

Proof. If $f \notin G$, then the right-hand side is infinite such that the bound trivially holds. Assuming $f \in G$, one has for any $\mathcal{T}_n \mathbf{x} \in V_n$

$$\begin{aligned} \|f - \mathcal{F}_{n,m}^{\text{RLS}} \mathbf{f}\|_H &\leq \|f - \mathcal{T}_n \mathbf{x}\|_H + \|\mathcal{T}_n \mathbf{x} - \mathcal{F}_{n,m}^{\text{RLS}} \mathbf{f}\|_H \\ &\leq \|f - \mathcal{T}_n \mathbf{x}\|_H + \frac{1}{\sqrt{A_{n,m}^\epsilon}} \sqrt{\|\mathcal{T}_n \mathbf{x} - \mathcal{F}_{n,m}^{\text{RLS}} \mathbf{f}\|_m^2 + p_\epsilon(\mathbf{x} - \mathcal{L}_{n,m}^{\text{RLS}} \mathbf{f})} \quad (\text{using (29)}) \\ &\leq \|f - \mathcal{T}_n \mathbf{x}\|_H + \frac{1}{\sqrt{A_{n,m}^\epsilon}} \left(\|\mathcal{T}_n \mathbf{x} - \mathcal{F}_{n,m}^{\text{RLS}} \mathbf{f}\|_m + \sqrt{p_\epsilon(\mathbf{x} - \mathcal{L}_{n,m}^{\text{RLS}} \mathbf{f})} \right). \end{aligned}$$

The second term can be bounded by

$$\|\mathcal{T}_n \mathbf{x} - \mathcal{F}_{n,m}^{\text{RLS}} \mathbf{f}\|_m \leq \|\mathcal{T}_n \mathbf{x} - f\|_m + \|f - \mathcal{F}_{n,m}^{\text{RLS}} \mathbf{f}\|_m \leq \|\mathcal{T}_n \mathbf{x} - f\|_m + \|\mathbf{f} - \mathcal{M}_m \mathcal{F}_{n,m}^{\text{RLS}} \mathbf{f}\|_2 + \|\mathbf{n}\|_2,$$

while the third term can be bounded by

$$\sqrt{p_\epsilon(\mathbf{x} - \mathcal{L}_{n,m}^{\text{RLS}} \mathbf{f})} \leq \sqrt{p_\epsilon(\mathbf{x})} + \sqrt{p_\epsilon(\mathcal{L}_{n,m}^{\text{RLS}} \mathbf{f})}$$

using the fact that $\sqrt{p_\epsilon}$ is subadditive and even. Combining these results we obtain

$$\begin{aligned} &\|\mathcal{T}_n \mathbf{x} - \mathcal{F}_{n,m}^{\text{RLS}} \mathbf{f}\|_m + \sqrt{p_\epsilon(\mathbf{x} - \mathcal{L}_{n,m}^{\text{RLS}} \mathbf{f})} \\ &\leq \|\mathcal{T}_n \mathbf{x} - f\|_m + \|\mathbf{f} - \mathcal{M}_m \mathcal{F}_{n,m}^{\text{RLS}} \mathbf{f}\|_2 + \|\mathbf{n}\|_2 + \sqrt{p_\epsilon(\mathbf{x})} + \sqrt{p_\epsilon(\mathcal{L}_{n,m}^{\text{RLS}} \mathbf{f})}, \\ &\leq (1 + \sqrt{2})(\|\mathcal{T}_n \mathbf{x} - f\|_m + \sqrt{p_\epsilon(\mathbf{x})} + \|\mathbf{n}\|_2), \end{aligned}$$

where in the second step (27) was used, more specifically,

$$\begin{aligned} &\|\mathbf{f} - \mathcal{M}_m \mathcal{F}_{n,m}^{\text{RLS}} \mathbf{f}\|_2^2 + p_\epsilon(\mathcal{L}_{n,m}^{\text{RLS}} \mathbf{f}) \leq \|\mathbf{f} - \mathcal{M}_m \mathcal{T}_n \mathbf{x}\|_2^2 + p_\epsilon(\mathbf{x}), \\ \Rightarrow &\|\mathbf{f} - \mathcal{M}_m \mathcal{F}_{n,m}^{\text{RLS}} \mathbf{f}\|_2 + \sqrt{p_\epsilon(\mathcal{L}_{n,m}^{\text{RLS}} \mathbf{f})} \leq \sqrt{2} \left(\|\mathbf{f} - \mathcal{M}_m \mathcal{T}_n \mathbf{x}\|_2 + \sqrt{p_\epsilon(\mathbf{x})} \right), \\ \Rightarrow &\|\mathbf{f} - \mathcal{M}_m \mathcal{F}_{n,m}^{\text{RLS}} \mathbf{f}\|_2 + \sqrt{p_\epsilon(\mathcal{L}_{n,m}^{\text{RLS}} \mathbf{f})} \leq \sqrt{2} \left(\|f - \mathcal{T}_n \mathbf{x}\|_m + \|\mathbf{n}\|_2 + \sqrt{p_\epsilon(\mathbf{x})} \right). \end{aligned}$$

The final result follows from $1 \leq \|\mathcal{M}_m\|_{G,2} < \infty$. \square

3.2 Discretizing numerically redundant spanning sets

We are specifically interested in ℓ^2 -regularization in order to compute accurate approximations in a numerically redundant spanning set. In this case, one has $p_\epsilon(\mathbf{x}) = \epsilon^2 \|\mathbf{x}\|_2^2$, such that the discretization condition becomes

$$A_{n,m}^\epsilon \|\mathcal{T}_n \mathbf{x}\|_H^2 \leq \|\mathcal{T}_n \mathbf{x}\|_m^2 + \epsilon^2 \|\mathbf{x}\|_2^2, \quad \forall \mathbf{x} \in \mathbb{C}^{n'}. \quad (31)$$

3.2.1 Absolute condition number

When using ℓ^2 -regularization, the operator $\mathcal{F}_{n,m}^{\text{RLS}}$ is linear. We can easily characterize its absolute condition number using $A_{n,m}^\epsilon$.

Theorem 8. *If (31) holds for some $A_{n,m}^\epsilon > 0$, then the absolute condition number of the regularized least squares operator $\mathcal{F}_{n,m}^{\text{RLS}}$ defined by (7) and (27) with $p_\epsilon(\mathbf{x}) = \epsilon^2 \|\mathbf{x}\|_2^2$ satisfies*

$$\kappa_{n,m}^{\text{RLS}} \leq \frac{1 + \sqrt{2}}{\sqrt{A_{n,m}^\epsilon}}.$$

Proof. Since $\mathcal{F}_{n,m}^{\text{RLS}}$ is a linear operator, one has

$$\begin{aligned} (\kappa_{n,m}^{\text{RLS}})^2 &= \sup_{\mathbf{d} \in \mathbb{C}^m} \frac{\|\mathcal{F}_{n,m}^{\text{RLS}} \mathbf{d}\|_H^2}{\|\mathbf{d}\|_2^2} \\ &\leq \left(\sup_{\mathbf{d} \in \mathbb{C}^m} \frac{\|\mathcal{F}_{n,m}^{\text{RLS}} \mathbf{d}\|_H^2}{\|\mathcal{F}_{n,m}^{\text{RLS}} \mathbf{d}\|_m^2 + \epsilon^2 \|\mathcal{L}_{n,m}^{\text{RLS}} \mathbf{d}\|_2^2} \right) \left(\sup_{\mathbf{d} \in \mathbb{C}^m} \frac{\|\mathcal{F}_{n,m}^{\text{RLS}} \mathbf{d}\|_m^2 + \epsilon^2 \|\mathcal{L}_{n,m}^{\text{RLS}} \mathbf{d}\|_2^2}{\|\mathbf{d}\|_2^2} \right), \end{aligned}$$

where $\mathcal{L}_{n,m}^{\text{RLS}}$ is defined by (27) with $p_\epsilon(\mathbf{x}) = \epsilon^2 \|\mathbf{x}\|_2^2$. The first factor can be bounded by $1/A_{n,m}^\epsilon$ using (31). To bound the second factor, note that following the definition of $\mathcal{L}_{n,m}^{\text{RLS}}$ one has

$$\|\mathbf{d} - \mathcal{M}_m \mathcal{F}_{n,m}^{\text{RLS}} \mathbf{d}\|_2^2 + \epsilon^2 \|\mathcal{L}_{n,m}^{\text{RLS}} \mathbf{d}\|_2^2 \leq \|\mathbf{d} - \mathcal{M}_m \mathcal{T}_n \mathbf{x}\|_2^2 + \epsilon^2 \|\mathbf{x}\|_2^2,$$

for all $\mathbf{x} \in \mathbb{C}^{n'}$. If we consider $\mathbf{x} = \mathbf{0}$, it follows that

$$\begin{aligned} \|\mathbf{d} - \mathcal{M}_m \mathcal{F}_{n,m}^{\text{RLS}} \mathbf{d}\|_2^2 + \epsilon^2 \|\mathcal{L}_{n,m}^{\text{RLS}} \mathbf{d}\|_2^2 &\leq \|\mathbf{d}\|_2^2 \\ \|\mathbf{d} - \mathcal{M}_m \mathcal{F}_{n,m}^{\text{RLS}} \mathbf{d}\|_2 + \epsilon \|\mathcal{L}_{n,m}^{\text{RLS}} \mathbf{d}\|_2 &\leq \sqrt{2} \|\mathbf{d}\|_2 && \text{(via } (a+b)^2 \leq 2(a^2 + b^2), \forall a, b \in \mathbb{R}^+) \\ \|\mathcal{M}_m \mathcal{F}_{n,m}^{\text{RLS}} \mathbf{d}\|_2 - \|\mathbf{d}\|_2 + \epsilon \|\mathcal{L}_{n,m}^{\text{RLS}} \mathbf{d}\|_2 &\leq \sqrt{2} \|\mathbf{d}\|_2 && \text{(reverse triangle inequality)} \\ \frac{\|\mathcal{F}_{n,m}^{\text{RLS}} \mathbf{d}\|_m + \epsilon \|\mathcal{L}_{n,m}^{\text{RLS}} \mathbf{d}\|_2}{\|\mathbf{d}\|_2} &\leq 1 + \sqrt{2} \\ \frac{\|\mathcal{F}_{n,m}^{\text{RLS}} \mathbf{d}\|_m^2 + \epsilon^2 \|\mathcal{L}_{n,m}^{\text{RLS}} \mathbf{d}\|_2^2}{\|\mathbf{d}\|_2^2} &\leq (1 + \sqrt{2})^2 && \text{(via } a^2 + b^2 \leq (a+b)^2, \forall a, b \in \mathbb{R}^+) \end{aligned}$$

□

3.2.2 Interpretation of the discretization condition

One might wonder how big the influence of the penalty term is for small ϵ . To this end, consider a numerically redundant spanning set Φ_n with frame bounds A_n and B_n , and choose $\epsilon = \epsilon_{\text{mach}} \|\mathcal{T}_n\|_{2,H} = \epsilon_{\text{mach}} \sqrt{B_n}$ for simplicity. Recall that the results of section 2.3 show that it should be taken slightly larger in practice. As follows from (19), the smallest nonzero singular value of \mathcal{T}_n is equal to $\sqrt{A_n}$. Using Property 1, this means that there exist $\mathbf{x} \in \mathbb{C}^{n'}$ for which

$$\|\mathcal{T}_n \mathbf{x}\|_H^2 = A_n \|\mathbf{x}\|_2^2 \leq \epsilon_{\text{mach}}^2 B_n \|\mathbf{x}\|_2^2 = \epsilon^2 \|\mathbf{x}\|_2^2$$

and, hence, for these sets of expansion coefficients (31) is automatically satisfied for $A_{n,m}^\epsilon = 1$. More generally, (31) is automatically satisfied for any $\mathbf{x} \in \mathbb{C}^{n'}$ satisfying $\|\mathcal{T}_n \mathbf{x}\|_H \leq \epsilon \|\mathbf{x}\|_2$. This reflects the idea that regularization makes the effective approximation space smaller. What happens in the case of an orthonormal spanning set? Such a set satisfies Parseval's identity: $\|\mathcal{T}_n \mathbf{x}\|_H = \|\mathbf{x}\|_2$. Therefore, (31) is equivalent to

$$(A_{n,m}^\epsilon - \epsilon^2) \|v\|_H^2 \leq \|v\|_m^2, \quad \forall v \in V_n, \quad (32)$$

which is a negligible relaxation compared to (9) for small ϵ . Hence, the penalty term only has a big influence on the discretization condition when Φ_n is numerically redundant.

In order to further illustrate the effect of the penalty term on the discretization condition, we present a simple example. Suppose one has a basis Φ_n and an associated sampling operator \mathcal{M}_m , and the basis is augmented with one extra function ψ . Typically, to ensure a good discretization, you would also need to enhance \mathcal{M}_m . However, if ψ can be approximated to machine precision within the span of Φ_n , it is intuitively clear that adding this extra function does not increase the approximation space “numerically”. In other words, the increase in approximation space obtained by adding an extra function to the spanning set is in such cases invisible on a computer with finite precision. This phenomenon is also discussed by Boyd in [15, section 16.6]. Consequently, it is also reasonable to expect that no additional samples are required. This intuition can be substantiated using (31), which takes into account the effects of finite precision. In general, (9) is not satisfied for the augmented basis, i.e., $A_{n,m} = 0$.

Lemma 1 (Augmented basis). *Given a basis Φ_n with $V_n = \text{span}(\Phi_n)$, and a sampling operator \mathcal{M}_m satisfying*

$$\|v\|_H^2 = \|v\|_m^2, \quad \forall v \in V_n. \quad (33)$$

Suppose we augment this basis with one additional function ψ . If

$$\inf_{v \in V_n} \|\psi - v\|_G \leq \epsilon / (\|\mathcal{M}_m\|_{G,2} + \sqrt{C_G}), \quad (34)$$

then

$$\frac{1}{2} \|\mathcal{T}\mathbf{x}\|_H^2 \leq \|\mathcal{T}\mathbf{x}\|_m^2 + \epsilon^2 \|\mathbf{x}\|_2^2, \quad \forall \mathbf{x} \in \mathbb{C}^{n+1}, \quad (35)$$

where \mathcal{T} is the synthesis operator associated with $\Phi_n \cup \{\psi\}$.

Proof. Define

$$\mathcal{T}\mathbf{x} = \sum_{i=1}^n x_i \phi_{i,n} + x_{n+1} \psi =: f + x_{n+1} \psi.$$

For any $g \in V_n$, it holds that

$$\|\mathcal{T}\mathbf{x}\|_H = \|f + x_{n+1} \psi\|_H \leq \|f + g\|_H + \|x_{n+1} \psi - g\|_H.$$

Furthermore, using (33),

$$\|f + g\|_H = \|f + g\|_m \leq \|f + x_{n+1} \psi\|_m + \|g - x_{n+1} \psi\|_m = \|\mathcal{T}\mathbf{x}\|_m + \|g - x_{n+1} \psi\|_m.$$

Hence,

$$\begin{aligned} \|\mathcal{T}\mathbf{x}\|_H &\leq \|\mathcal{T}\mathbf{x}\|_m + \|x_{n+1} \psi - g\|_m + \|x_{n+1} \psi - g\|_H \\ \|\mathcal{T}\mathbf{x}\|_H &\leq \|\mathcal{T}\mathbf{x}\|_m + (\|\mathcal{M}_m\|_{G,2} + \sqrt{C_G}) \|x_{n+1} \psi - g\|_G. \end{aligned}$$

Since the above holds for any $g \in V_n$, it follows from (34) that

$$\|\mathcal{T}\mathbf{x}\|_H \leq \|\mathcal{T}\mathbf{x}\|_m + \epsilon |x_{n+1}|.$$

Using $(a+b)^2 \leq 2(a^2 + b^2)$, this leads to

$$\|\mathcal{T}\mathbf{x}\|_H^2 \leq (\|\mathcal{T}\mathbf{x}\|_m + \epsilon |x_{n+1}|)^2 \leq 2(\|\mathcal{T}\mathbf{x}\|_m^2 + \epsilon^2 |x_{n+1}|^2) \leq 2(\|\mathcal{T}\mathbf{x}\|_m^2 + \epsilon^2 \|\mathbf{x}\|_2^2). \quad \square$$

3.2.3 Common methods for ℓ^2 -regularization

The choice $p_\epsilon(\mathbf{x}) = \epsilon^2 \|\mathbf{x}\|_2^2$ is also known as Tikhonov regularization. Another popular method for ℓ^2 -regularization is the truncated singular value decomposition (TSVD). This type of regularization slightly differs from Tikhonov regularization, yet a near-optimal solution is returned in the following sense: for any input data $\mathbf{d} \in \mathbb{C}^m$ the computed coefficients $\mathcal{L}_{n,m} \mathbf{d}$ satisfy

$$\|\mathbf{d} - \mathcal{M}_m \mathcal{T}_n \mathcal{L}_{n,m} \mathbf{d}\|_2 + \epsilon \|\mathcal{L}_{n,m} \mathbf{d}\|_2 \leq C_{\mathcal{L}} (\|\mathbf{d} - \mathcal{M}_m \mathcal{T}_n \mathbf{x}\|_2 + \epsilon \|\mathbf{x}\|_2), \quad \forall \mathbf{x} \in \mathbb{C}^{n'}, \quad (36)$$

for some $C_{\mathcal{L}} \geq 1$. With only a minor adjustment to the proof of Theorem 7, it follows immediately that the approximation error can be bounded by

$$\|f - \mathcal{F}_{n,m} \mathbf{f}\|_H \leq \left(\sqrt{C_G} + \frac{(1 + C_{\mathcal{L}}) \|\mathcal{M}_m\|_{G,2}}{\sqrt{A_{n,m}^\epsilon}} \right) e_n^\epsilon(f) + \frac{1 + C_{\mathcal{L}}}{\sqrt{A_{n,m}^\epsilon}} \|\mathbf{n}\|_2. \quad (37)$$

For completeness, we show that TSVD regularization indeed satisfies (36). The same result follows from combining [20, Lemma 3.3] and [6, Theorem 3.8].

Lemma 2 (TSVD regularization). *The operator*

$$\mathcal{L}_{n,m}^{TSVD} : \mathbb{C}^m \rightarrow \mathbb{C}^{n'}, \quad \mathbf{d} \mapsto (\mathcal{M}_m \mathcal{T}_n)_\epsilon^\dagger \mathbf{d},$$

where $(\cdot)_\epsilon^\dagger$ denotes the Moore-Penrose inverse after truncation of the singular values below a threshold ϵ , satisfies (36) for $C_{\mathcal{L}} = 2$.

Proof. Define $T := \mathcal{M}_m \mathcal{T}_n$. It holds that

$$\begin{aligned} T(T)_\epsilon^\dagger &= \sum_i \mathbf{u}_i \sigma_i \mathbf{v}_i^* \sum_{\sigma_i \geq \epsilon} \mathbf{v}_i \frac{1}{\sigma_i} \mathbf{u}_i^* = \sum_{\sigma_i \geq \epsilon} \mathbf{u}_i \mathbf{u}_i^*, \\ (T)_\epsilon^\dagger T &= \sum_{\sigma_i \geq \epsilon} \mathbf{v}_i \frac{1}{\sigma_i} \mathbf{u}_i^* \sum_i \mathbf{u}_i \sigma_i \mathbf{v}_i^* = \sum_{\sigma_i \geq \epsilon} \mathbf{v}_i \mathbf{v}_i^*, \end{aligned}$$

where \mathbf{u}_i , σ_i and \mathbf{v}_i are the left singular vectors, singular values and right singular vectors of T , respectively. Hence, $T(T)_\epsilon^\dagger$ and $(T)_\epsilon^\dagger T$ are orthogonal projections onto $\text{span}(\{\mathbf{u}_i \mid \sigma_i \geq \epsilon\})$ and $\text{span}(\{\mathbf{v}_i \mid \sigma_i \geq \epsilon\})$, respectively. Using $\mathbf{d} = (\mathbf{d} - T\mathbf{x}) + T\mathbf{x}$, $\forall \mathbf{x} \in \mathbb{C}^{n'}$, it follows from here that

$$\begin{aligned} \|\mathbf{d} - T(T)_\epsilon^\dagger \mathbf{d}\|_2 &= \|(I - T(T)_\epsilon^\dagger)((\mathbf{d} - T\mathbf{x}) + T\mathbf{x})\|_2 \\ &\leq \|I - T(T)_\epsilon^\dagger\|_{2,2} \|\mathbf{d} - T\mathbf{x}\|_2 + \|(I - T(T)_\epsilon^\dagger)T\|_{2,2} \|\mathbf{x}\|_2, \\ &\leq \|\mathbf{d} - T\mathbf{x}\|_2 + \epsilon \|\mathbf{x}\|_2, \end{aligned}$$

where $I : \mathbb{C}^m \rightarrow \mathbb{C}^m$ is the identity operator. Similarly,

$$\begin{aligned} \epsilon \|(T)_\epsilon^\dagger \mathbf{d}\|_2 &= \epsilon \|(T)_\epsilon^\dagger ((\mathbf{d} - T\mathbf{x}) + T\mathbf{x})\|_2 \\ &\leq \epsilon \|(T)_\epsilon^\dagger\|_{2,2} \|\mathbf{d} - T\mathbf{x}\|_2 + \epsilon \|(T)_\epsilon^\dagger T\|_{2,2} \|\mathbf{x}\|_2, \\ &\leq \|\mathbf{d} - T\mathbf{x}\|_2 + \epsilon \|\mathbf{x}\|_2. \end{aligned}$$

□

4 Random sampling for L^2 -approximations

The question naturally arises: how can one construct a sampling operator that satisfies the regularized norm inequality (31)? To address this question, we draw inspiration from the unregularized case. Recently, Cohen and Migliorati [19] introduced an elegant strategy to generate random pointwise samples that satisfy (9) for least squares fitting. This approach, reviewed in section 4.1, is closely related to the concept of *leverage scores*, which are used to subsample tall-and-skinny matrices in a fully discrete setting. Leverage score sampling is a well-established technique in numerical linear algebra and machine learning. Moreover, an extension of leverage scores, known as *ridge leverage scores*, has been developed specifically for regularized settings. Using a continuous analogue of these scores, we present a sampling strategy for ℓ^2 -regularized function approximation in section 4.2. In section 4.3, a general framework is given for the analysis of the effects of regularization given a numerically redundant spanning set. Throughout the whole section, we work under the mild assumption that for any \mathbf{x} in the domain of V_n , there exists a $v \in V_n$ such that $v(\mathbf{x}) \neq 0$.

4.1 Results without regularization

In [18, 19] random sampling for discrete least squares approximation of unknown functions $f : X \rightarrow \mathbb{R}$ living in $H = L^2(X, d\rho)$ is analysed, where $X \subset \mathbb{R}^d$ and ρ is a given probability measure on X . The analysis is based on the observation that the norm inequality (9) is equivalent to a spectral bound

$$A_{n,m} G_n \preceq G_{n,m}, \quad (38)$$

where \preceq denotes the Loewner order. Here, $G_{n,m}$ and G_n are the discrete and continuous Gram matrices representing the operators $(\mathcal{M}_m \mathcal{U}_n)^* (\mathcal{M}_m \mathcal{U}_n)$ and $\mathcal{U}_n^* \mathcal{U}_n$, respectively, where \mathcal{U}_n is the synthesis operator associated with any set of functions Ψ_n satisfying $\text{span}(\Psi_n) = V_n$. We stress that this equivalence holds for any such set Ψ_n , not only for the chosen spanning set Φ_n (1). However, if one considers an orthonormal set $\Psi_n = \{\psi_i\}_{i=1}^n$, the analysis simplifies significantly. In this case, one has $G_n = I$ and $A_{n,m}$ is simply related to the smallest eigenvalue of $G_{n,m}$.

As explained in [19, Proof of Theorem 2.1], suppose one uses a sampling operator \mathcal{M}_m based on random pointwise samples

$$l_{j,m} : f \mapsto \sqrt{w(\mathbf{x}_j)/mf(\mathbf{x}_j)}, \quad \mathbf{x}_j \stackrel{\text{iid}}{\sim} \mu, \quad (39)$$

where the sampling measure $d\mu$ and weight function w satisfy $w d\mu = d\rho$. Then, $G_{n,m}$ can be written as $\sum_{j=1}^m X_j$ where X_j are i.i.d. copies of the random matrix $X(\mathbf{x})$ with

$$(X(\mathbf{x}))_{k,l} := \frac{1}{m} w(\mathbf{x}) \overline{\psi_k(\mathbf{x})} \psi_l(\mathbf{x}), \quad k, l = 1 \dots n,$$

where \mathbf{x} is distributed according to μ . The smallest eigenvalue of $G_{n,m}$ can now be bounded from below with high probability using a matrix concentration bound that solely depends on the number of samples m and the maximum of the quantity

$$\|X(\mathbf{x})\|_2 = \frac{1}{m} w(\mathbf{x}) \sum_{i=1}^n |\psi_i(\mathbf{x})|^2 = \frac{1}{m} w(\mathbf{x}) k_n(\mathbf{x}),$$

where we defined

$$k_n(\mathbf{x}) := \sum_{i=1}^n |\psi_i(\mathbf{x})|^2. \quad (40)$$

This definition assumes that Ψ_n is orthonormal. However, it is independent of the specific choice of the orthonormal set Ψ_n ; the function k_n only depends on $V_n = \text{span}(\Psi_n)$ and the probability density ρ . The function k_n has been analysed in the field of classical analysis long before its introduction in the analysis of discrete least squares problems. In classical analysis, it is known as the inverse of the *Christoffel function* [42]. Furthermore, its discrete analogue is known as *leverage scores*, which are widely used in randomized numerical linear algebra and machine learning, see e.g. [39, §2].

This reasoning led to the following sampling result, which is a restatement of [23, Lemma 2.1].

Theorem 9. [23, Lemma 2.1] *Consider the sampling operator \mathcal{M}_m defined by the sampling functionals (39). Let $\gamma > 0$ and*

$$m \geq 9.25 \|wk_n\|_{L^\infty(X)} \log(2n/\gamma), \quad (41)$$

then (9) is satisfied for $A_{n,m} = 1/2$ with probability at least $1 - \gamma$.

Can we optimize the sampling distribution μ such that the required number of samples in Theorem 9 is minimized? The following key observation was first highlighted in [19]. Observe that $\{\sqrt{w}\psi_i\}_{i=1}^n$ is an $L^2(X, d\mu)$ orthonormal basis for $\sqrt{w}V_n$ and, therefore, $\int_X w(\mathbf{x}) k_n(\mathbf{x}) d\mu = n$. As a consequence, we know that $\|wk_n\|_{L^\infty(X)} \geq n$. Consider now the sampling distribution

$$w(\mathbf{x}) = \frac{n}{k_n(\mathbf{x})}, \quad \text{such that} \quad d\mu = \frac{k_n(\mathbf{x})}{n} d\rho. \quad (42)$$

This sampling distribution satisfies $\|wk_n\|_{L^\infty(X)} = n$ and, hence, minimizes the right-hand side of (41). One can easily check that (42) indeed describes a probability density since $\int_X k_n(\mathbf{x}) d\rho = n$ and $k_n(\mathbf{x}) > 0$.

Corollary 1. *Consider the sampling operator \mathcal{M}_m defined by the sampling functionals (39) with $d\mu$ as defined by (42). Let $\gamma > 0$ and*

$$m \geq 9.25n \log(2n/\gamma),$$

then (9) is satisfied for $A_{n,m} = 1/2$ with probability at least $1 - \gamma$.

It follows that the sampling distribution (42) requires only $\mathcal{O}(n \log(n))$ samples for accurate least squares fitting with high probability. As a result, the amount of required data is nearly optimal, where “optimal” corresponds to the case of interpolation with $m = n$. For a summary of optimality benchmarks and probabilistic error analyses, we refer to [23, section 1 and 2]. Also, we note that considerable efforts have been made to obtain $\mathcal{O}(n)$ sampling strategies, see e.g. [1, section 8] and references therein.

4.2 Introducing ℓ^2 -regularization

We now turn to random sampling for discrete ℓ^2 -regularized least squares approximations to unknown functions $f : X \rightarrow \mathbb{R}$ living in $H = L^2(X, d\rho)$. Analogously to (38), observe that (31) is equivalent to

$$A_{n,m} G_n \preceq G_{n,m} + \epsilon^2 I. \quad (43)$$

An important difference compared to section 4.1 is the dependence on the chosen spanning set Φ_n . In this case, we are bound to the choice $\Psi_n = \Phi_n$, i.e., G_n and $G_{n,m}$ represent the operators $(\mathcal{M}_m \mathcal{T}_n)^*(\mathcal{M}_m \mathcal{T}_n)$ and $\mathcal{T}_n^* \mathcal{T}_n$, respectively, where \mathcal{T}_n is the synthesis operator associated with the spanning set Φ_n .

Similar spectral bounds have been analysed before in the setting of randomized algorithms [9, 10, 11, 44] using analogous techniques as the ones described in section 4.1. In this case, a continuous analogue of the ϵ -ridge leverage scores [9, Definition 1] is of interest

$$k_n^\epsilon(\mathbf{x}) := \sum_{i=1}^n \frac{\sigma_i^2}{\sigma_i^2 + \epsilon^2} |u_i(\mathbf{x})|^2, \quad (44)$$

where σ_i and $u_i(\mathbf{x})$ are the singular values and left singular vectors, evaluated at \mathbf{x} , associated with the synthesis operator \mathcal{T}_n . We refer to (44) as the inverse of the *effective Christoffel function*. The following properties are easily derived: $k_n^0 = k_n$ and $k_n^\epsilon \leq k_n$. Furthermore, whereas k_n solely depends on the subspace V_n and the $L^2(X, d\rho)$ -norm, k_n^ϵ also depends on the chosen spanning set Φ_n and the regularization parameter ϵ . Another important difference is that $\int_X k_n(\mathbf{x}) d\rho = n$, but

$$\int_X k_n^\epsilon(\mathbf{x}) d\rho = \sum_{i=1}^n \frac{\sigma_i^2}{\sigma_i^2 + \epsilon^2} =: n^\epsilon. \quad (45)$$

In the discrete context, the quantity n^ϵ is referred to as the *effective dimension* [9]. It satisfies $n^\epsilon \leq n$ and it is a decreasing function of the regularization parameter ϵ .

Using very similar techniques as [10, proof of Lemma 6], we can prove the following sampling result. The reworked proof can be found in Appendix B.

Theorem 10. *Consider the sampling operator \mathcal{M}_m defined by the sampling functionals (39). Assuming $\epsilon > 0$ and $\|G_n\|_2 \geq \epsilon^2$, let $\gamma \in (0, 1)$ and*

$$m \geq \frac{32}{3} \|wk_n^\epsilon\|_{L^\infty(X)} \log(16n^\epsilon/\gamma),$$

then (31) is satisfied for $A_{n,m}^\epsilon = 1/2$ with probability at least $1 - \gamma$.

Following a similar reasoning as in section 4.1, we again consider the sampling distribution with

$$w(\mathbf{x}) = \frac{n^\epsilon}{k_n^\epsilon(\mathbf{x})}, \quad \text{such that} \quad d\mu = \frac{k_n^\epsilon(\mathbf{x})}{n^\epsilon} d\rho. \quad (46)$$

It follows from $\int_X k_n^\epsilon(\mathbf{x}) d\rho = n^\epsilon$ that (46) is indeed a well-defined sampling distribution.

Corollary 2. *Consider the sampling operator \mathcal{M}_m defined by the sampling functionals (39) with $d\mu$ as defined by (46). Assuming $\epsilon > 0$ and $\|G_n\|_2 \geq \epsilon^2$, let $\gamma \in (0, 1)$ and*

$$m \geq \frac{32}{3} n^\epsilon \log(16n^\epsilon/\gamma),$$

then (31) is satisfied for $A_{n,m}^\epsilon = 1/2$ with probability at least $1 - \gamma$.

It is worthwhile to interpret the differences between the results laid out in section 4.1 and those in this section. Using Theorem 1, it follows that the sampling strategy proposed in Corollary 1 results in a least squares approximation with

$$\|f - \mathcal{F}_{n,m}^{\text{LS}} \mathbf{f}\|_H \leq C \inf_{v \in V_n} \|f - v\|_G \quad (47)$$

using

$$m \geq Cn \log(n) \quad (48)$$

samples, with high probability and assuming the data \mathbf{f} is noiseless. On the other hand, it follows from Theorem 2 that the sampling strategy proposed in Corollary 2 results in a regularized least squares approximation with

$$\|f - \mathcal{F}_{n,m}^{\text{RLS}} \mathbf{f}\|_H \leq C \inf_{\mathbf{x} \in \mathbb{C}^{n'}} \|f - \mathcal{T}_n \mathbf{x}\|_G + \epsilon \|\mathbf{x}\|_2 \quad (49)$$

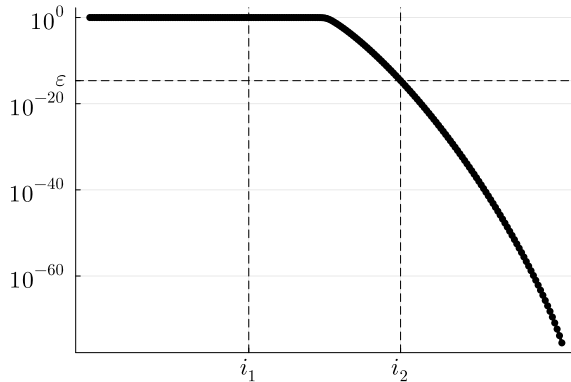


Figure 1: A typical singular value profile of the synthesis operator \mathcal{T}_n associated with a subsequence (21) of a linearly independent overcomplete frame with frame bounds $A = B = 1$. The singular value profile can be analysed by splitting it in three regions, where $\sigma_i^2 \geq 1 - \epsilon^2$ for $i \leq i_1$ and $\sigma_i^2 \leq \epsilon^2$ for $i > i_2$. The region in between i_1 and i_2 is often referred to as the plunge region.

using

$$m \geq Cn^\epsilon \log(n^\epsilon) \quad (50)$$

samples, again with high probability and assuming the data \mathbf{f} is noiseless. In these statements the constant $C > 0$ is generic and may change with each occurrence. These results demonstrate that regularization generally decreases the achievable accuracy, yet also decreases the amount of data required to obtain a near-best approximation. Furthermore, the effective dimension n^ϵ in regularized approximations serves a similar role as the dimension n in unregularized approximations.

Two important remarks are to be made. First, as discussed in section 2, optimality in the sense of (47) is unattainable when computing with a numerically redundant spanning set on a machine with finite precision. Additionally, section 6 demonstrates that straightforward numerical orthogonalization of the spanning set does not mitigate the effects of finite precision. As a result, optimality in the sense of (49) is the best one can aim for in this case. Second, in practice one typically has $n^\epsilon = \mathcal{O}(n)$ such that (48) and (50) are asymptotically equivalent as $n \rightarrow \infty$. This suggests that the gain in data efficiency achieved through regularization is generally limited to a constant factor when samples are drawn from the optimal distributions proposed in Corollary 1 and 2. However, one cannot always choose which distribution to sample from. Since k_n can differ significantly from k_n^ϵ , the required number of samples drawn from a specific distribution μ may vary considerably depending on whether or not the effects of regularization are accounted for, as described in Theorems 9 and 10. This phenomenon is illustrated further on in section 5.2.2 for a Fourier extension frame.

4.3 Behaviour of n^ϵ and k_n^ϵ

For approximation with numerically redundant spanning sets, we are specifically interested in the setting where ϵ is of the order of a finite working precision ϵ_{mach} associated with the numerical computations. It is natural to wonder whether this has a big influence, i.e., whether the effective degrees of freedom n^ϵ differ significantly from n and the behaviour of k_n^ϵ differs significantly from the behaviour of k_n , for small regularization parameters ϵ .

Following [5] and section 2, numerically redundant spanning sets Φ_n that form a subsequence of a linearly independent overcomplete frame Ψ are of particular interest. For these sets, regularized approximations are guaranteed to converge down to ϵ_{mach} accuracy, see e.g. Theorem 4. As discussed in section 2.1, the singular values of the synthesis operator associated with such spanning sets lie within $[A_n, B_n]$, where $A_n \rightarrow 0$ as $n \rightarrow \infty$ and $B_n < B$. Here, A_n and B_n denote the frame bounds of Φ_n , and B denotes the upper frame bound of the infinite-dimensional frame Ψ . Figure 1 illustrates a typical singular value profile of a synthesis operator \mathcal{T}_n associated with a spanning set that is a subsequence of a frame Ψ with $A = B = 1$. Notably, whereas the spectrum of the synthesis operator associated with Ψ is contained within $\{0\} \cup [A, B]$, the finite synthesis operator \mathcal{T}_n has spurious eigenvalues in $(0, A)$, which arise due to spectral pollution [22].

One can split the singular value profile into different regimes, by identifying i_1 and i_2 such that

$$\sigma_i^2 \geq 1 - \epsilon^2 \text{ for } i \leq i_1 \quad (51)$$

and

$$\sigma_i^2 \leq \epsilon^2 \text{ for } i > i_2. \quad (52)$$

The region in between i_1 and i_2 is often referred to as the *plunge region* [21]. These regions have a different influence on the effective degrees of freedom n^ϵ and the maximum of the inverse effective Christoffel function k_n^ϵ , as quantified in the following theorem.

Theorem 11. *Given i_1 and i_2 satisfying (51) and (52), then*

$$n^\epsilon \leq i_2 + S_{\text{tail}} \quad (53)$$

and

$$\frac{1}{2} k_n^{\text{trunc}}(\mathbf{x}) \leq k_n^\epsilon(\mathbf{x}) \leq k_n^{\text{trunc}}(\mathbf{x}) + S_{\text{tail}} \max_{i_2 < i \leq n} |u_i(\mathbf{x})|^2, \quad (54)$$

where $S_{\text{tail}} = \sum_{i=i_2+1}^n (\sigma_i/\epsilon)^2$ and $k_n^{\text{trunc}}(\mathbf{x}) = \sum_{i=1}^{i_2} |u_i(\mathbf{x})|^2$. Furthermore, if Φ_n is linearly independent and uniformly bounded, $\|\phi_{i,n}\|_{L^\infty(X)} \leq 1$ ($1 \leq i \leq n$), then

$$\|k_n^\epsilon\|_{L^\infty(X)} \leq \frac{n}{1 - \epsilon^2} + ((i_2 - i_1) + S_{\text{tail}}) \max_{i_1 < i \leq n} \|u_i\|_{L^\infty(X)}^2. \quad (55)$$

Proof. Equation (53) follows immediately from splitting the summation that defines n^ϵ as

$$n_\epsilon = \sum_{i=1}^n \frac{\sigma_i^2}{\sigma_i^2 + \epsilon^2} = \sum_{i=1}^{i_2} \frac{\sigma_i^2}{\sigma_i^2 + \epsilon^2} + \sum_{i=i_2+1}^n \frac{\sigma_i^2}{\sigma_i^2 + \epsilon^2} \leq \sum_{i=1}^{i_2} 1 + \sum_{i=i_2+1}^n \frac{\sigma_i^2}{\epsilon^2} = i_2 + S_{\text{tail}}.$$

For (54), consider

$$k_n^{\text{trunc}}(\mathbf{x}) = \sum_{i=1}^{i_2} |u_i(\mathbf{x})|^2 \leq 2 \sum_{i=1}^{i_2} \frac{\sigma_i^2}{\sigma_i^2 + \epsilon^2} |u_i(\mathbf{x})|^2 \leq 2 \sum_{i=1}^n \frac{\sigma_i^2}{\sigma_i^2 + \epsilon^2} |u_i(\mathbf{x})|^2 = 2k_n^\epsilon(\mathbf{x})$$

and

$$k_n^\epsilon(\mathbf{x}) = \sum_{i=1}^n \frac{\sigma_i^2}{\sigma_i^2 + \epsilon^2} |u_i(\mathbf{x})|^2 \leq \sum_{i=1}^{i_2} |u_i(\mathbf{x})|^2 + \sum_{i=i_2+1}^n \frac{\sigma_i^2}{\epsilon^2} |u_i(\mathbf{x})|^2 \leq k_n^{\text{trunc}}(\mathbf{x}) + S_{\text{tail}} \max_{i_2 < i \leq n} |u_i(\mathbf{x})|^2.$$

In order to obtain (55), we split the above as

$$\begin{aligned} \|k_n^\epsilon\|_{L^\infty(X)} &\leq \sup_{\mathbf{x} \in X} \left(\sum_{i=1}^{i_1} |u_i(\mathbf{x})|^2 + \sum_{i=i_1+1}^{i_2} |u_i(\mathbf{x})|^2 + S_{\text{tail}} \max_{i_2 < i \leq n} |u_i(\mathbf{x})|^2 \right) \\ &\leq \sup_{\mathbf{x} \in X} \sum_{i=1}^{i_1} |u_i(\mathbf{x})|^2 + ((i_2 - i_1) + S_{\text{tail}}) \max_{i_1 < i \leq n} \|u_i\|_{L^\infty(X)}^2. \end{aligned}$$

The first term can be bounded using the singular value decomposition of \mathcal{T}_n

$$\sum_{i=1}^{i_1} |u_i(\mathbf{x})|^2 = \|w(\mathbf{x})VD^{-1}\|_2^2 \leq \|w(\mathbf{x})\|_2^2 \|V\|_2^2 \|D^{-1}\|_2^2 = \frac{\|w(\mathbf{x})\|_2^2}{\sigma_{i_1}^2} \leq \frac{\|w(\mathbf{x})\|_2^2}{1 - \epsilon^2},$$

where $w(\mathbf{x}) = [\phi_{1,n}(\mathbf{x}) \ \dots \ \phi_{n,n}(\mathbf{x})]$, $V \in \mathbb{C}^{n \times i_1}$ is a matrix with orthogonal columns and $D \in \mathbb{C}^{i_1 \times i_1}$ is a diagonal matrix with $(D)_{(i,i)} = \sigma_i$. The final result follows from

$$\sup_{\mathbf{x} \in X} \frac{\|w(\mathbf{x})\|_2^2}{1 - \epsilon^2} \leq \frac{1}{1 - \epsilon^2} \sup_{\mathbf{x} \in X} \sum_{i=1}^n |\phi_{i,n}(\mathbf{x})|^2 \leq \frac{1}{1 - \epsilon^2} \sum_{i=1}^n \|\phi_{i,n}\|_{L^\infty(X)}^2 \leq \frac{n}{1 - \epsilon^2}.$$

□

Foremost, it becomes clear that regularization decreases the importance of small singular values and the associated basis functions u_i . For the effective degrees of freedom, it follows from Theorem 11 that $S_{\text{tail}} = \sum_{i=i_2+1}^n (\sigma_i/\epsilon)^2$ is an important quantity. This quantity heavily depends on the decay of the singular values. For instance, if they are exponentially decaying with a rate that is independent of n , one has $S_{\text{tail}} \leq C$ for varying n . In this case, the effective degrees of freedom scale with i_2 . In practice, the decay of the singular values typically has a minor dependence on n , see e.g. section 5.2.1, such that S_{tail} grows slowly with n . Furthermore, we find that the basis functions u_i associated with small singular values indeed have a smaller impact on (54) and (55) than those associated to large singular values. This effect can be considerable, as illustrated in section 5.2.2 for the Fourier extension frame, where $k_n = \mathcal{O}(n^2)$ while $k_n^\epsilon = \mathcal{O}(n \log(n))$.

The reasoning above could give the impression that the behaviour of the basis functions u_i associated to small singular values ($i > i_2$) is insignificant. According to (54) this is not generally true; only if these functions are sufficiently bounded, the inverse effective Christoffel function k_n^ϵ is guaranteed to behave like the inverse Christoffel function k_n^{trunc} associated to the set $\{u_i\}_{i=1}^{i_2}$. In the discrete setting, the latter is often referred to as the *leverage scores associated to the best rank- i_2 space* [9]. This distinction is important for practical purposes, since k_n^{trunc} is computable to high accuracy using ϵ_{mach} precision, while computing k_n^ϵ and k_n requires extended precision.

5 Applications

5.1 Approximating with known asymptotic behaviour

An approximation problem typically stems from an underlying problem in science or engineering, where expert knowledge on its solution is often available. It is, however, non-trivial to incorporate this knowledge into an efficient numerical scheme. One way to do this is by adding extra basis functions to the spanning set, which capture the known properties of the function to be approximated. This forces us to compute with non-standard bases that are often numerically redundant. For instance, suppose our goal is to approximate

$$f(x) = J_{1/2}(x+1) + \frac{1}{x^2+1}, \quad x \in [-1, 1] \quad (56)$$

where $J_{1/2}$ denotes the Bessel function of the first kind of order 1/2. It is known from asymptotic analysis that $J_{1/2}(x+1) \sim \sqrt{x+1}$ as $x \rightarrow -1$, which can be taken into account by working with a spanning set

$$\Phi_n = \{\varphi_i\}_{i=1}^{n/2} \cup \{\psi_i\}_{i=1}^{n/2}, \quad \text{where } \psi_i = w\varphi_i, \quad (57)$$

assuming n is even. The functions φ_i are standard (smooth) basis functions, while the singular behaviour is represented by the weight function w . For $w \in L^\infty(-1, 1)$, this spanning set is a subsequence of an overcomplete linearly independent frame with frame bounds $A = 1 + \text{ess inf}_{x \in (-1, 1)} |w(x)|^2$ and $B = 1 + \text{ess sup}_{x \in (-1, 1)} |w(x)|^2$ [5, Example 3]. Hence, following section 2.1, Φ_n is numerically redundant for sufficiently large n . For further analysis and usecases of this type of spanning sets we refer to [5] and references therein. For the approximation of f (56), we choose φ_i equal to the Legendre polynomial of degree $i-1$ and $w(x) = \sqrt{(x+1)}/2$. In this case, Φ_n is a subsequence of a frame with frame bounds $A = 1$ and $B = 2$.

5.1.1 Properties of Φ_n

On Figure 2, the approximation of f (56) for three different spanning sets is shown: Legendre polynomials, monomials, and the Legendre + Weighted Legendre spanning set defined by (57). Figures 2a and 2b display the first eight elements of the spanning sets along with the singular value profile of their associated synthesis operator for $n = 100$. The Legendre basis functions are orthonormal, such that all singular values of the synthesis operator are equal to 1. In contrast, the monomials and the Legendre + Weighted Legendre spanning set are both numerically redundant for sufficiently large n . However, a clear qualitative difference exists between these two sets. As can be seen on Fig. 2a, the monomials look increasingly more alike as their degree increases, such that high-degree monomials are indistinguishable when using finite precision. As a result, all singular values of the synthesis operator

are exponentially decaying. The Legendre + Weighted Legendre spanning set contains half of the Legendre basis augmented with weighted Legendre functions. Hence, in contrast to the monomial basis, a large portion of the set is well-distinguishable. As a result, the synthesis operator has many singular values $\sigma_i \approx 1$, combined with exponentially decaying singular values. This matches the singular value profile described in section 4.3.

On Fig. 2c and 2d, the L^2 -norm of the approximation error and the L^2 -norm of the expansion coefficients are displayed for the approximation of f using a truncated singular value decomposition (TSVD) solver with $\epsilon = 10\epsilon_{\text{mach}}^{\text{dp}}$, where $\epsilon_{\text{mach}}^{\text{dp}}$ denotes the working precision associated with IEEE double precision floating point numbers. The approximations are computed using 5000 Legendre points. Both the Legendre basis and the monomials span the space of polynomials up to degree $n - 1$ and, therefore, theoretically exhibit the same algebraic rate of convergence for the approximation of f . However, the expansion coefficients of the monomial approximations blow up, such that the error of the numerically computed approximation stagnates, following the results of section 2.2. On the other hand, the approximation in the Legendre + weighted Legendre spanning set converges exponentially. The norm of the expansion coefficients initially grows, yet expansions with modest coefficient exist as $n \rightarrow \infty$, guaranteeing accurate numerical approximations. This is to be expected, since Φ_n is a subsequence of an infinite-dimensional linearly independent frame, see e.g. Theorem 4.

5.1.2 Deterministic sampling

Deterministic sample sets can be analysed by identifying the largest $A_{n,m}^\epsilon$ for which the norm inequality

$$A_{n,m}^\epsilon \|\mathcal{T}_n \mathbf{x}\|_H^2 \leq \|\mathcal{T}_n \mathbf{x}\|_m^2 + \epsilon^2 \|\mathbf{x}\|_2^2, \quad \forall \mathbf{x} \in \mathbb{C}^n$$

holds. An error bound on the discrete regularized least squares approximation then follows from Theorem 2. Observe that one can determine $A_{n,m}^\epsilon$ by computing the smallest generalized eigenvalue λ of

$$(G_{n,m} + \epsilon^2 I) \mathbf{v} = \lambda G_n \mathbf{v}, \quad (58)$$

where $G_{n,m}$ and G_n represent the operators $(\mathcal{M}_m \mathcal{T}_n)^* (\mathcal{M}_m \mathcal{T}_n)$ and $\mathcal{T}_n^* \mathcal{T}_n$, respectively. We compare this to the largest $A_{n,m}$ for which the norm inequality

$$A_{n,m} \|v\|_H^2 \leq \|v\|_m^2, \quad \forall v \in V_n$$

holds, which corresponds to the smallest generalized eigenvalue λ of

$$G_{n,m} \mathbf{v} = \lambda G_n \mathbf{v}. \quad (59)$$

The constant $A_{n,m}$ results in an error bound on the discrete least squares approximation via Theorem 1.

How should one choose sample points for approximation in the spanning set defined by (57)? Intuitively, it is clear that we need sample points related to the smooth behaviour of φ_i and sample points related to the singular behaviour of w . For the first we use Legendre points, while for the latter we use sample points that are exponentially clustered towards $x = -1$. Using a structured point set such as Legendre points is advantageous as it creates structured subblocks within the discrete least squares matrix. This structure can be exploited to increase the computational efficiency of solving the least squares problem, as demonstrated by the AZ algorithm for frame approximations [20, 30]. Moreover, exponentially clustered points have been found effective for least squares approximation of functions with branch point singularities [32].

The two-parameter plots on Figure 3 show $1/\sqrt{A_{m,n}}$, $1/\sqrt{A_{m,n}^\epsilon}$, and the uniform approximation error of the TSVD approximation to $f = J_{1/2}(x+1) + 1/(x^2+1)$ in Φ_n (57) with $n = 80$, for a varying number of Legendre points and exponentially clustered sample points. The regularization parameter equals $\epsilon = 10\epsilon_{\text{mach}}^{\text{dp}}$, where $\epsilon_{\text{mach}}^{\text{dp}}$ denotes the working precision associated with IEEE double precision floating point numbers. From Figure 2c, we know that the best approximation to f in the Legendre + weighted Legendre spanning set is of the order of machine precision. Following Theorem 1 and Theorem 2, both $1/\sqrt{A_{m,n}}$ and $1/\sqrt{A_{m,n}^\epsilon}$ give an indication of the error of the discrete least squares approximation. From the numerical results, we conclude that $A_{n,m}^\epsilon$ accurately predicts the behaviour of the uniform approximation error, while $A_{n,m}$ overestimates the amount of samples that are needed for accurate numerical approximation.

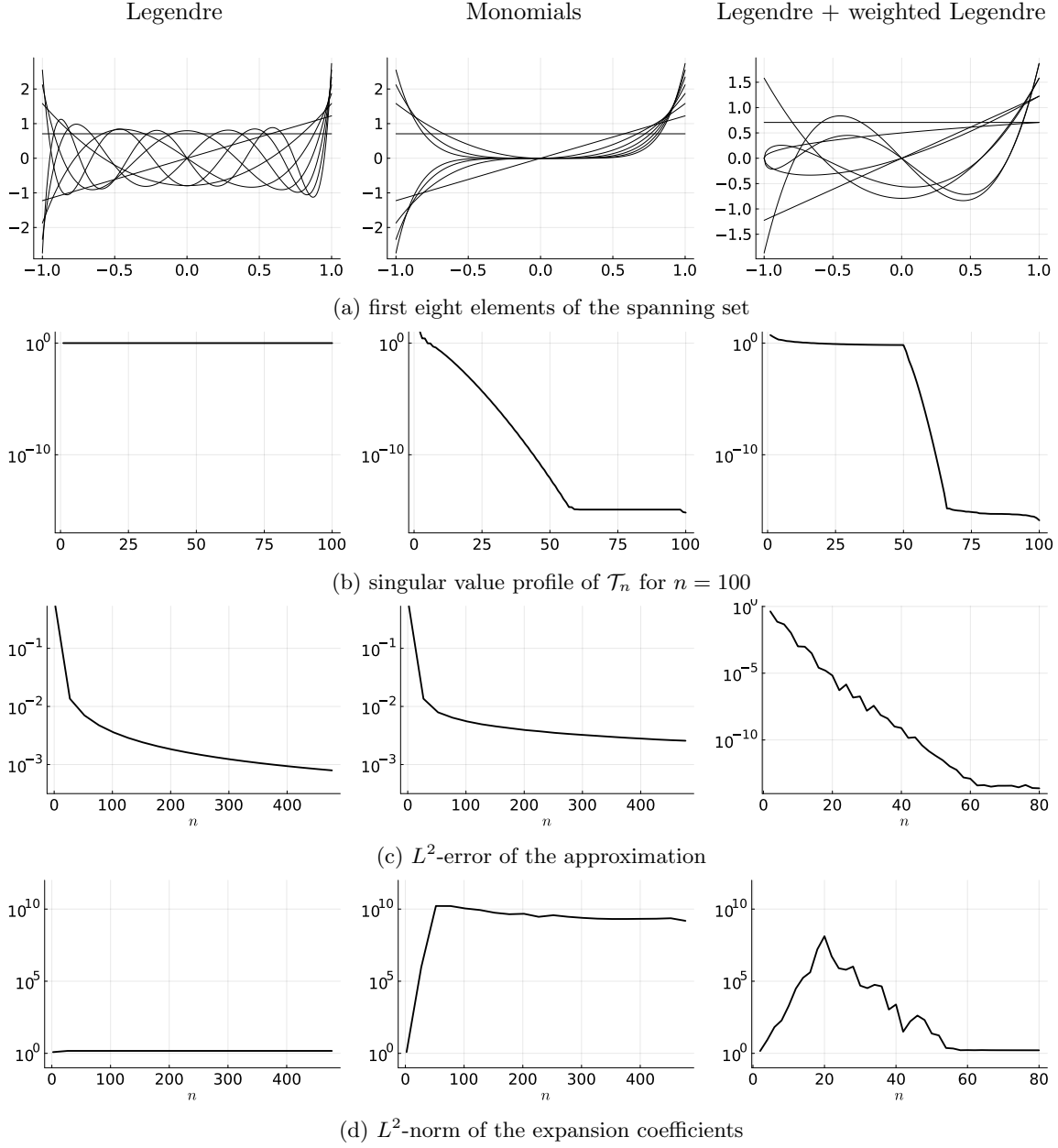


Figure 2: Comparison between approximating with Legendre polynomials up to degree $n-1$, monomials up to degree $n-1$ and the Legendre + weighted Legendre spanning set defined by (57) for the approximation of $f(x) = J_{1/2}(x+1) + 1/(x^2+1)$ using a TSVD solver with $\epsilon = 10 \epsilon_{\text{mach}}^{\text{dp}}$.

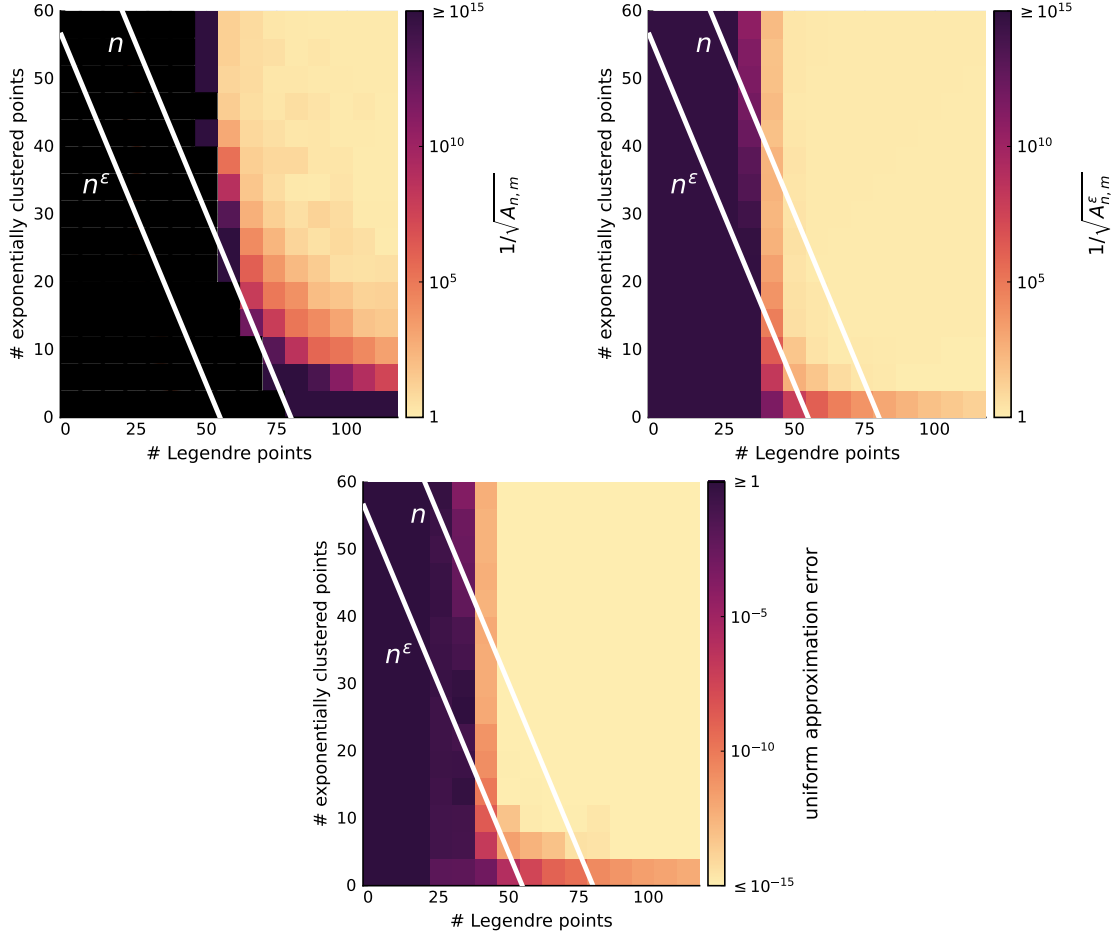


Figure 3: Analysis of the Legendre + weighted Legendre spanning set defined by (57) for $n = 80$. Left: $1/\sqrt{A_{n,m}}$, right: $1/\sqrt{A_{n,m}^\epsilon}$ for $\epsilon = 10 \epsilon_{\text{mach}}^{\text{dp}} \approx 2 \times 10^{-15}$, bottom: the uniform approximation error of the TSVD approximation of $f(x) = J_{1/2}(x+1) + 1/(x^2+1)$ with truncation threshold ϵ . The black squares correspond to $A_{n,m} = 0$. The white lines mark when the total number of samples equals $n = 80$ or $n^\epsilon \approx 54.8$, the effective degrees of freedom. We conclude that $A_{n,m}^\epsilon$ accurately predicts the behaviour of the approximation error, while $A_{n,m}$ overestimates the amount of samples that are needed for accurate numerical approximation.

5.2 Approximating on irregular domains

Approximating a function on an irregular domain $D \subset \mathbb{R}^d$ is required for many computational problems, yet an orthonormal or Riesz basis is generally unknown for such a domain. Therefore, numerical methods often resort to working with an orthonormal basis defined on a bounding box surrounding D . Crucially, this set of functions does not form an orthonormal basis for the underlying domain D , but it does constitute an overcomplete frame, referred to as an *extension frame*. As discussed in section 2.1, a subsequence of an overcomplete frame inevitably becomes numerically redundant as its size increases and, hence, regularization is needed for numerical stability. Approximating on an irregular domain is, therefore, a typical scenario in which numerical redundancy arises. An alternative strategy is to compute with a numerically orthogonalized spanning set. However, section 6 shows that straightforward techniques to orthogonalize do not succeed in circumventing the effects of finite precision, and result in approximations that behave similarly as regularized approximations.

As a toy example for the behaviour of extension frames, we will analyse a one-dimensional Fourier extension frame. More specifically, for approximation on $[-W, W]$ with $W < 1/2$ one can use the Fourier basis on the extension $[-1/2, 1/2]$, i.e.,

$$\phi_{k,n} = \exp(2\pi i x k), \quad -(n-1)/2 \leq k \leq (n-1)/2 \quad (60)$$

for odd n . Smooth functions, not necessarily periodic on $[-W, W]$, can be approximated in $V_n = \text{span}(\Phi_n)$ with exponential convergence [35]. As mentioned before, regularization is needed for numerical stability, and lowers the accuracy of the approximation. The numerical convergence behaviour is extensively analysed in [7].

In this section, we analyse how regularization affects the required amount of data for accurate approximation using the results from section 4, which focus on random pointwise sampling. The associated analysis outlined in section 4.3 depends heavily on a good understanding of the singular values and the singular vectors associated to the synthesis operator \mathcal{T}_n . For many spanning sets, little is known about this; however, the singular vectors of the Fourier extension frame are related to discrete prolate spheroidal wave functions (DPSWFs), which have been analysed extensively in the field of signal processing. For a detailed explanation of this connection, see [38, section 3.1]. DPSWFs are an indispensable tool for bandlimited extrapolation, introduced and thoroughly analysed by Slepian and his collaborators during their time at Bell Labs [46]. In this setting, a notion of effective degrees of freedom is not new, see e.g. [37] and [21, section 2.3]

5.2.1 Effective degrees of freedom

In the case of pointwise random sampling, the required number of samples for accurate regularized least squares approximation scales with $n^\epsilon \log(n^\epsilon)$, as stated in Theorem 10. Here, n^ϵ denotes the effective degrees of freedom. This theorem assumes that the samples are drawn randomly from a (near-)optimal sampling distribution defined by (46). The effective degrees of freedom n^ϵ thus play a similar role for regularized approximation as the dimension n for unregularized approximation. The following theorem formalizes the dependence of n^ϵ on n , W and ϵ for the one-dimensional Fourier extension frame.

Theorem 12. *For the spanning set defined by (60),*

$$i_2 = \lceil 2nW \rceil + 2 + \frac{2}{\pi^2} \log\left(\frac{8}{\epsilon^2}\right) \log(4n) \quad (61)$$

satisfies (52). For this choice of i_2 , one has

$$S_{\text{tail}} \leq \frac{2}{\pi^2} \log(4n) \quad (62)$$

such that the effective degrees of freedom n^ϵ can be bounded by

$$n^\epsilon \leq \lceil 2nW \rceil + 2 + \frac{2}{\pi^2} \left(\log\left(\frac{8}{\epsilon^2}\right) + 1 \right) \log(4n). \quad (63)$$

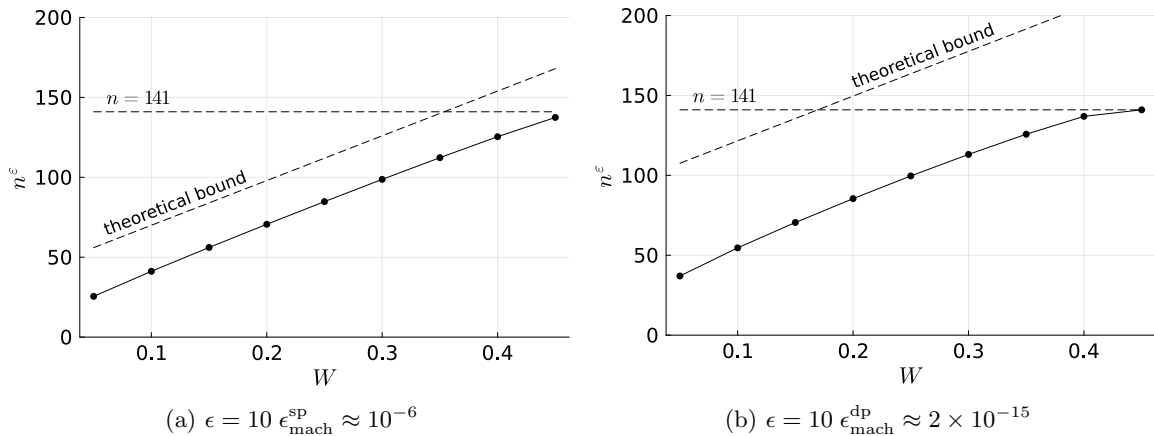


Figure 4: The effective degrees of freedom n^ϵ for the one-dimensional Fourier extension frame (60) as a function of the domain parameter W , for $n = 141$. The dashed lines illustrate $n^\epsilon \leq n = 141$ and the theoretical bound $n^\epsilon \leq \lceil 2nW \rceil + 2 + \frac{2}{\pi^2} (\log(8/\epsilon^2) + 1) \log(4n)$ stated in Theorem 12.

Proof. Note that $\sigma_i(\mathcal{T}_n)^2$ equals the i -th eigenvalue of the Gram matrix G_n , representing the operator $\mathcal{T}_n^* \mathcal{T}_n$. Furthermore, G_n is exactly the *prolate matrix* [36, eq. (1)]. Therefore, $\sigma_i(\mathcal{T}_n)^2 = \lambda_{i-1}$, for all $i = 1, \dots, n$, where the latter is analysed in [36]. It follows from [36, Corollary 1] that (52) holds for (61). Moreover, (62) can be deduced by [36, Corollary 2]. The final result is a consequence of Theorem 11. \square

A numerical verification of Theorem 12 is shown on Figure 4 for $n = 141$ and $\epsilon = 10 \epsilon_{\text{mach}}^{\text{sp}} \approx 10^{-6}$ and $\epsilon = 10 \epsilon_{\text{mach}}^{\text{dp}} \approx 2 \times 10^{-15}$, where $\epsilon_{\text{mach}}^{\text{sp}}$ and $\epsilon_{\text{mach}}^{\text{dp}}$ denote the working precision associated with IEEE single and double precision floating point numbers, respectively. Note that the computation of n^ϵ is done in extended precision, such that the singular values σ_i can be computed with a working precision significantly smaller than ϵ . For implementational details, we refer to [31]. Both the theory and the numerical verification show that the effective degrees of freedom essentially scale as $2nW$. This formalizes the intuition that increased redundancy, i.e., smaller W , results in a reduced amount of required information. Observe that $n^\epsilon = \mathcal{O}(n)$, such that asymptotically the amount of samples needed for regularized and unregularized approximation is similar, namely $\mathcal{O}(n \log(n))$.

5.2.2 Uniformly random sampling

For many applications, one cannot freely choose the sample distribution. Another interesting question to answer in this regard is how many uniformly random samples are needed for accurate approximation. As follows from Theorems 9 and 10 for $w = 1$, this number is proportional to the maximum of the inverse Christoffel function k_n and the inverse effective Christoffel function k_n^ϵ for unregularized and regularized least squares fitting, respectively. The following theorem shows that $\|k_n\|_{L^\infty[-W,W]} = \mathcal{O}(n^2)$.

Theorem 13. *For the spanning set defined by (60), the maximum of the inverse Christoffel function k_n can be bounded by*

$$C_1 \left(\left(1 + \frac{\pi}{2}\right) n^2 - \pi/2 \right) \leq \|k_n\|_{L^\infty[-W,W]} \leq C_2 \left(\left(1 + \frac{\pi}{2}\right) n^2 - \pi/2 \right),$$

where $C_1, C_2 > 0$ are independent of n .

Proof. An alternative characterization of the inverse Christoffel function [42, eq. (4.1.1)] is

$$k_n(x) = \max_{v \in V_n} \frac{|v(x)|^2}{\|v\|_{L^2[-W,W]}^2}, \quad \text{such that} \quad \|k_n\|_{L^\infty[-W,W]} = \max_{v \in V_n} \frac{\|v\|_{L^\infty[-W,W]}^2}{\|v\|_{L^2[-W,W]}^2}.$$

From [26, Theorem 1] it immediately follows that there exist constants $C_1, C_2 > 0$ such that

$$C_1 \left(\left(1 + \frac{\pi}{2}\right) n^2 - \pi/2 \right) \leq \max_{v \in V_n} \frac{\|v\|_{L^\infty[-W,W]}^2}{\|v\|_{L^2[-W,W]}^2} \leq C_2 \left(\left(1 + \frac{\pi}{2}\right) n^2 - \pi/2 \right).$$

□

The effective inverse Christoffel function k_n^ϵ can be bounded using (55), which depends on the size of the plunge region $i_2 - i_1$ and S_{tail} . The latter is shown to be $\mathcal{O}(\log(n))$ in Theorem 12. The following theorem proves that the size of the plunge region is $\mathcal{O}(\log(n))$ as well.

Theorem 14. *For the spanning set defined by (60),*

$$i_1 = \lfloor 2nW \rfloor - 1 - \frac{2}{\pi^2} \log\left(\frac{8}{\epsilon^2}\right) \log(4n) \quad (64)$$

satisfies (51). Moreover, the maximum of k_n^ϵ can be bounded by

$$\|k_n^\epsilon\|_{L^\infty[-W,W]} \leq \frac{n}{1 - \epsilon^2} + \left(4 + \frac{2}{\pi^2} \left(2 \log\left(\frac{8}{\epsilon^2}\right) + 1\right) \log(4n)\right) \max_{i_1 < i \leq n} \|u_i\|_{L^\infty[-W,W]}^2. \quad (65)$$

Proof. Similarly as for the proof of Theorem 12, observe that $\sigma_i(\mathcal{T}_n)^2 = \lambda_{i-1}$, for all $i = 1, \dots, n$, where the latter is analysed in [36]. It follows from [36, Corollary 1] that (51) holds for (64). By combining the results from Theorem 12 with (55) and (64), we arrive at (65). □

It remains to examine how the basis functions u_i behave. As mentioned before, these functions are linked to the discrete prolate spheroidal wave functions. In Appendix C, we summarize known asymptotic results due to Slepian, which indicate that $\|u_i\|_{L^\infty[-W,W]} = \mathcal{O}(\sqrt{n})$ as $n \rightarrow \infty$ for all i , such that

$$\|k_n^\epsilon\|_{L^\infty[-W,W]} = \mathcal{O}(n \log(n)).$$

This behaviour is verified numerically in Figure 5, which confirms that $\|k_n\|_{L^\infty[-W,W]} = \mathcal{O}(n^2)$, while $\|k_n^\epsilon\|_{L^\infty[-W,W]}$ appears to grow linearly in n . This difference translates in the need for log-linear or quadratic oversampling when computing a least squares approximation with or without regularization, respectively, using uniformly random samples.

As an example, we approximate $f = 1/(1 - 0.32x)$ on $[-W, W]$ with $W = 0.3$ in the Fourier extension frame defined by (60) using uniformly random samples. The approximation is computed using a truncated singular value decomposition (TSVD) solver with threshold $\epsilon = 10 \epsilon_{\text{mach}}^{\text{dp}} \approx 2 \times 10^{-15}$, where $\epsilon_{\text{mach}}^{\text{dp}}$ denotes the working precision associated with IEEE double precision floating point numbers. Figure 6 shows the L^2 -error and demonstrates that linear oversampling suffices for convergence down to machine precision. In contrast, if we were to analyse this problem without taking regularization into account, we would conclude from Theorem 13 that quadratic oversampling is needed.

The approximation seems to converge root-exponentially. For a more detailed analysis of the convergence behaviour, we refer to [7]. Note that convergence is exponential without regularization, see e.g. [35] and the example in section 6, but demands quadratic oversampling. Hence, we get root-exponential convergence as a function of the number of sample points m with and without regularization. This is an example of a setting where the negative effects of regularization, i.e., reduced accuracy, are balanced by the positive effects, i.e., reduced need for data. What happens if we want to compute an approximation that converges root-exponentially all the way down to zero? In this case, we would need to vary the precision and the regularization parameter with n : $\epsilon \sim \epsilon_{\text{mach}} = \exp(-C\sqrt{n})$ for some $C > 0$. Following Theorem 14, linear oversampling does not suffice in this case. Specifically, the required linear oversampling factor scales with $\log(1/\epsilon)$.

As discussed for the Legendre + weighted Legendre basis in section 5.1.2, it is often preferred to use structured point sets, as they allow for the design of efficient least squares solvers such as the AZ algorithm for frame approximations [20, 30]. However, the analysis of deterministic sample sets is significantly more involved than that of random samples. An extensive analysis of equispaced sample points for polynomial extension frames is presented in [8], which arrives at a very similar conclusion.

6 Implicit regularization in numerical orthogonalization

It might be tempting to avoid working with numerically redundant spanning sets by simply orthogonalizing them. Indeed, several computational methods work with a numerically orthogonalized basis, for example [40, 23]. How do these methods compare to the regularized least squares method analysed

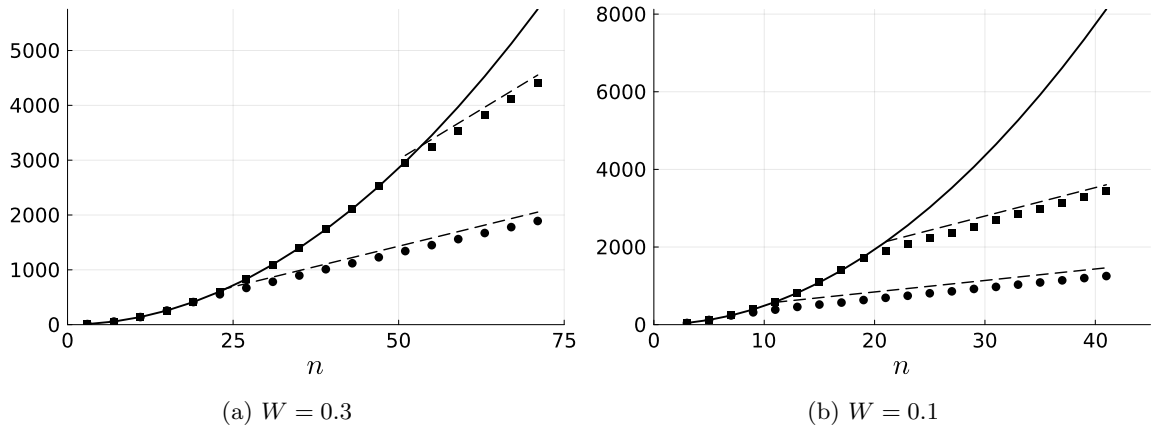


Figure 5: The maximum of the inverse (effective) Christoffel function for the one-dimensional Fourier extension frame (60) as a function of n . Full line: $\|k_n\|_{L^\infty[-W,W]}$, circles: $\|k_n^\epsilon\|_{L^\infty[-W,W]}$ for single precision $\epsilon = 10^{-6}$, and squares: $\|k_n^\epsilon\|_{L^\infty[-W,W]}$ for double precision $\epsilon = 2 \times 10^{-15}$. The linear behaviour of k_n^ϵ versus the quadratic behaviour of k_n implies a difference between log-linear and quadratic sampling rates for least squares fitting with uniformly random samples. The dashed lines mark $5 \log_{10}(1/\epsilon) + C$, for varying constant C . They empirically match the behaviour of k_n^ϵ .

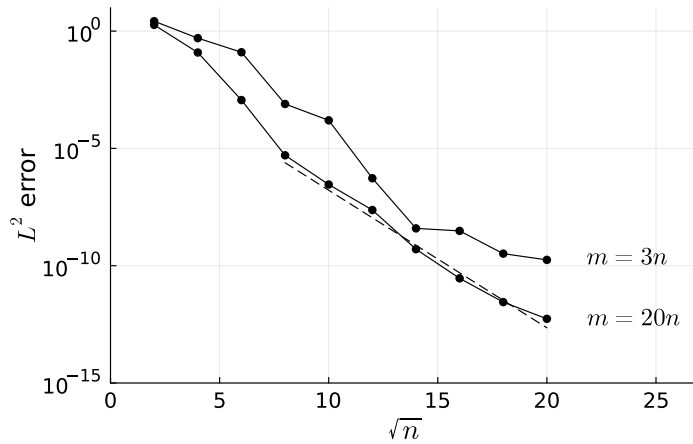


Figure 6: Error of the TSVD approximation of $f = 1/(1 - 0.32x)$ in the Fourier extension frame defined by (60) for $W = 0.3$, using m uniformly random samples and a truncation threshold $\epsilon = 10^{-15}$. The figure illustrates that linear oversampling suffices for convergence down to machine precision. In contrast, an analysis that ignores the effects of regularization would suggest a need for quadratic oversampling. The approximation appears to converge root-exponentially, while convergence without regularization is exponential but demands quadratic oversampling. Thus, root-exponential convergence as a function of the number of sample points m occurs both with and without regularization. This is an example of a setting where the negative effects of regularization, i.e., reduced accuracy, are balanced by the positive effects, i.e., reduced need for data.

in this paper? Are they substantially different? In this section, we show that regularization is implicitly present in straightforward numerical orthogonalization techniques. We aim to convey the main ideas, though each pointer provided in this section deserves further exploration. Note that Theorem 3 also suggests that it is impossible to orthogonalize a set numerically without suffering from the effects associated with finite precision.

6.1 Three orthogonalization strategies

For simplicity, we assume that a set of linearly independent functions $\{\eta_1, \dots, \eta_n\}$ is given, which spans the approximation space V_n with $\dim(V_n) = n$. One straightforward way of orthogonalizing consists of discretizing these functions on a fine grid $\{\mathbf{t}_j\}_{j=1}^l$ and computing a factorization

$$\begin{bmatrix} \eta_1(\mathbf{t}_1)/\sqrt{l} & \dots & \eta_n(\mathbf{t}_1)/\sqrt{l} \\ \vdots & & \vdots \\ \eta_1(\mathbf{t}_l)/\sqrt{l} & \dots & \eta_n(\mathbf{t}_l)/\sqrt{l} \end{bmatrix} = A = QR, \quad (66)$$

where $Q \in \mathbb{C}^{l \times n}$ is orthonormal and $R \in \mathbb{C}^{n \times n}$ is full rank, for example via QR decomposition or singular value decomposition. A new basis $\{\tilde{\eta}_1, \dots, \tilde{\eta}_n\}$ can then be obtained by solving

$$[\tilde{\eta}_1 \dots \tilde{\eta}_n] R = [\eta_1 \dots \eta_n]. \quad (67)$$

This basis is orthogonal with respect to the discrete inner product defined by $\langle f, g \rangle_l = (1/l) \sum_{j=1}^l f(\mathbf{t}_j) \overline{g(\mathbf{t}_j)}$. If the grid $\{\mathbf{t}_j\}_{j=1}^l$ is sufficiently dense, the functions are also (approximately) orthonormal with respect to the inner product associated with the Hilbert space H . The basis $\{\tilde{\eta}_j\}_{j=1}^n$ can then be used as a spanning set $\Phi_n = \{\phi_{i,n}\}_{i=1}^n$ (1) for least squares approximation.

Importantly, in the case of a numerically redundant set of functions $\{\eta_1, \dots, \eta_n\}$, the matrices A and R are heavily ill-conditioned. More specifically, their singular value profiles mimic that of the synthesis operator associated with $\{\eta_1, \dots, \eta_n\}$, having very small yet nonzero singular values. Can (67) even be computed with high accuracy in such cases? As an example, we consider the QR decomposition as a factorization method for (66), such that R is upper-triangular. The accuracy of solving triangular systems of equations is analysed extensively in [33], which shows that the solution can be surprisingly accurate despite ill-conditioning. The key insight is that the forward error depends on the Skeel condition number [45]:

$$\kappa_\infty^s(R) = \| |R^{-1}| |R| \|_\infty \leq \kappa_\infty(R) = \|R^{-1}\|_\infty \|R\|_\infty, \quad (68)$$

where $|\cdot|$ denotes the operation of replacing each element by its absolute value. We illustrate in the next section that the Skeel condition number can also grow very large for numerically redundant sets. Hence, accuracy is not guaranteed. It is often hidden in practice that (67) is solved with low accuracy, since standard routines such as Matlab's `backslash` succeed without any warning. However, due to the severe ill-conditioning of R , some form of regularization is necessarily used when computing (67) and, hence, the effects discussed in this paper come into play.

An alternative to computing $\{\eta_1, \dots, \eta_n\}$ explicitly using (67) consists of working with the sampled basis

$$Q = \begin{bmatrix} \tilde{\eta}_1(\mathbf{t}_1)/\sqrt{l} & \dots & \tilde{\eta}_n(\mathbf{t}_1)/\sqrt{l} \\ \vdots & & \vdots \\ \tilde{\eta}_1(\mathbf{t}_l)/\sqrt{l} & \dots & \tilde{\eta}_n(\mathbf{t}_l)/\sqrt{l} \end{bmatrix}.$$

In this case, we do not have to solve an ill-conditioned linear system; however, we can only access the basis $\{\tilde{\eta}_1, \dots, \tilde{\eta}_n\}$ on the grid $\{\mathbf{t}_j\}_{j=1}^l$. For an algorithm implemented in finite precision, it can only be guaranteed that the computed matrices \hat{Q} and \hat{R} factor the matrix A with a small backward error. As an example, we consider the Householder QR algorithm, which is analysed in [34, section 19.3]. Following [34, p.361], one has

$$A + \Delta A = \hat{Q} \hat{R}, \quad \text{with} \quad \|\Delta a_j\|_2 \leq C \epsilon_{\text{mach}} \|a_j\|_2, \quad (69)$$

where C is a constant that depends on the dimensions of the problem and the working precision ϵ_{mach} . Because of the small singular values of A , the range of $A + \Delta A$, and consequently the range of \hat{Q} , can

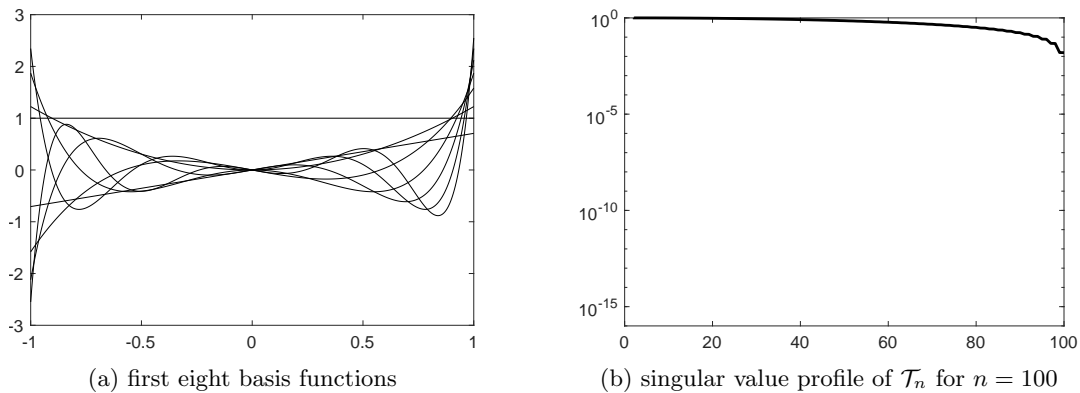


Figure 7: The Arnoldi basis associated with Stieltjes orthogonalization / the Vandermonde with Arnoldi algorithm along with the singular value profile of the associated synthesis operator. This set of functions has well behaved frame bounds, i.e., B_n/A_n is small, in contrast to the monomials displayed in Figure 2a and 2b. Hence, the set is not numerically redundant and can be numerically orthogonalized without suffering from the effects of finite precision.

differ significantly from that of A . A toy example confirming this statement is given in [47, p. 263], and a study of the angle between the subspaces $R(A)$ and $R(A + \Delta A)$ is given in [25]. In conclusion, there are no guarantees that the computed basis functions span the complete approximation space V_n . Observe the similarity between (69) and, for example, TSVD regularization: the range of \hat{Q} contains the singular vectors of A associated with large singular values $\sigma_i \gg \epsilon_{\text{mach}}$, yet the directions associated to small singular values can be perturbed or even absent. This implies that the best approximation still cannot be computed.

Finally, there exist algorithms that do succeed in computing an orthonormal basis for the whole approximation space V_n , seemingly starting from a numerically redundant set. These methods typically use some additional analytic knowledge. One example is the Stieltjes procedure for generating orthogonal polynomials [27], which recently gained popularity for numerical polynomial approximations in the form of the Vandermonde with Arnoldi (VwA) algorithm [16]. The algorithm is built on the simple principle that multiplying a polynomial by x increases its degree. The orthogonalization procedure can be summarized by the following Matlab code, using Chebfun [24]:

```

T_v = chebfun('1'); x = chebfun('x'); T_u = T_v/norm(T_v);
for i = 2:n
    % new Arnoldi iteration = multiplication by x
    v = x*T_u(:,end);
    T_v = [T_v v];
    % orthogonalize against previous functions
    v = v - T_u*pinv(T_u)*v;
    T_u = [T_u v/norm(v)];
end

```

Most importantly, the algorithm does not actually orthogonalize monomials. Instead, new “Arnoldi” basis functions, stored in T_v , are iteratively created to be better suited for orthogonalization. Indeed, the algorithm does not orthogonalize x^i , but x times the previous orthonormal basis function. On Figure 7, the first eight of these Arnoldi basis functions are plotted, along with the singular value profile of the synthesis operator associated with this basis for $n = 100$. Compare this to Figure 2a and 2b. The synthesis operator associated with the Arnoldi basis is much better conditioned than the synthesis operator of the monomials. This phenomenon is analysed for a variety of domains in [48]. We remark that the VwA algorithm performs discrete orthogonalization. Furthermore, the algorithm can be extended to other sets of functions provided they have similar Vandermonde-like system matrices A (66), as illustrated in the example below.

6.2 A numerical example

As an illustration, the different methods mentioned above are compared numerically. To this end, we reproduce [16, Example 3]. More specifically, we approximate the function $f(x) = 1/(10 - 9x)$ on $[-1, 1]$ using a Fourier extension on $[-2, 2]$, i.e.,

$$f(x) \approx \sum_{k=-n}^n c_k \exp(ik\pi x/2).$$

Since f is real, this can be simplified to

$$f(x) \approx \operatorname{Re} \left(\sum_{k=0}^n x_k \exp(ik\pi x/2) \right).$$

On [16, Fig. 5.1], a comparison is shown between the direct computation of a least squares fit using Matlab's `backslash` and the Vandermonde with Arnoldi (VwA) algorithm. The computations are based on function evaluations in 1000 Chebyshev points. Note that VwA is applicable in this setting, since the discrete least squares matrix has Vandermonde structure as described in [16, Example 3]. It is also important to remark that Matlab's `backslash` implicitly computes a regularized least squares approximation due to the numerical rank-deficiency of the discrete least squares matrix.

We add some extra methods to the comparison: approximation using a numerically orthogonalized basis obtained via a QR decomposition as described above, and a truncated singular value (TSVD) approximation. For implementational details, we refer to [16] and [31]. The results are presented in Figure 8. The VwA algorithm achieves exponential convergence, which is to be expected in $\operatorname{span}(\Phi_n)$ [35]. On the other hand, the accuracy of both the regularized and the numerically orthogonalized approximations decreases compared to the theoretical convergence behaviour around $n = 20$. This example confirms that straightforward numerical orthogonalization techniques implicitly regularize the approximation problem.

Figure 9 shows the singular value profile of the synthesis operator associated with Φ_n for $n = 10$ (left), $n = 20$ (middle), and $n = 30$ (right), computed in double precision using Chebfun [24]. Without rounding errors, the singular values would proceed to decrease exponentially toward zero as n goes to infinity. From the frame bounds A_n and B_n of Φ_n , one can infer that Φ_n becomes numerically redundant around $n = 20$. As shown in Figure 8, this is the exact point where the influence of regularization on the convergence behaviour becomes significant.

Perpendicular to the question of how to obtain an orthonormal basis, one might wonder what the advantages and disadvantages are of approximation with an orthonormalized spanning set (for example, using the VwA algorithm) compared to regularized approximation with a redundant spanning set. Most importantly, as illustrated in Figure 8, regularization typically slows down convergence. On the other hand, orthogonalizing often throws away exploitable structure. More specifically, the discrete least squares matrix associated with Φ_n in the example above is a submatrix of a Fourier matrix. This structure can be exploited to design efficient least squares methods, see for example the AZ algorithm for frames approximations [20, 30], or to allow for cheaper evaluation of the approximation. Furthermore, regularization also lowers the number of measurements that are needed for accurate approximation, which is exactly the focus of this paper.

A Accuracy of backward stable algorithms

Proof of Theorem 5. For any linear operator $\Delta\mathcal{T}_n$ mapping from $\mathbb{C}^{n'}$ to H and any $\Delta f \in H$, we have that

$$\|f - \mathcal{T}_n \hat{\mathbf{c}}\|_H \leq \|(f + \Delta f) - (\mathcal{T}_n + \Delta\mathcal{T}_n) \hat{\mathbf{c}}\|_H + \|\Delta f\|_H + \|\Delta\mathcal{T}_n \hat{\mathbf{c}}\|_H.$$

Since $\hat{\mathbf{c}}$ is computed by a backward stable algorithm with stability constant C , there exist $\hat{\Delta}\mathcal{T}_n$ and $\hat{\Delta}f$ satisfying $\|\hat{\Delta}\mathcal{T}_n\|_{2,H} \leq C \epsilon_{\text{mach}} \|\mathcal{T}_n\|_{2,H}$ and $\|\hat{\Delta}f\|_H \leq C \epsilon_{\text{mach}} \|f\|_H$ such that

$$\hat{\mathbf{c}} \in \arg \min_{\mathbf{x} \in \mathbb{C}^{n'}} \|(f + \hat{\Delta}f) - (\mathcal{T}_n + \hat{\Delta}\mathcal{T}_n) \mathbf{x}\|_H.$$

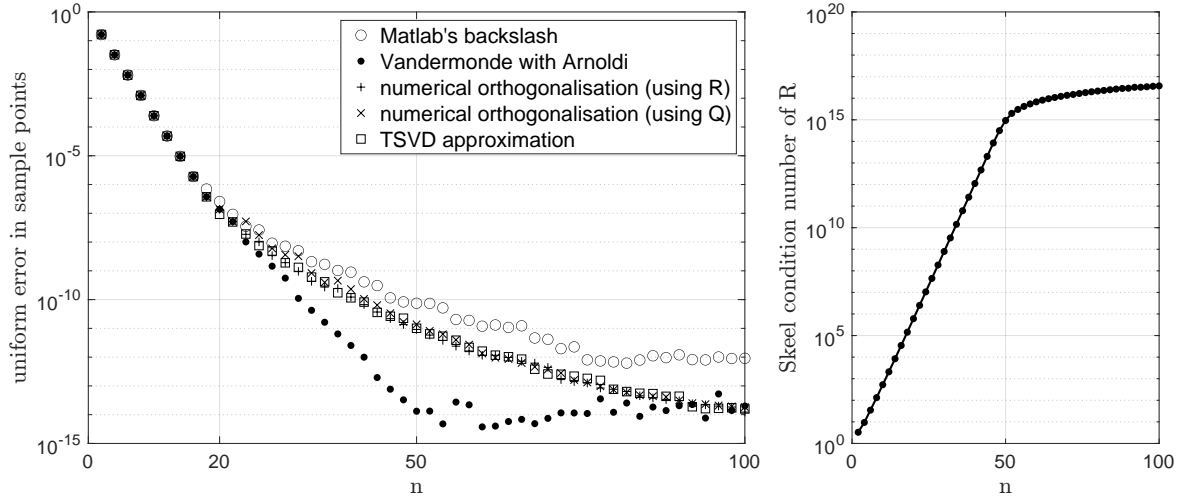


Figure 8: Approximation of $f(x) = 1/(10-9x)$ using a Fourier extension on $[-2, 2]$. Left: a comparison between a regularized least squares approximation using Matlab's `backslash`, the Vandermonde with Arnoldi algorithm, least squares approximation using a numerically orthogonalized basis obtained via a QR decomposition, and a TSVD approximation, right: the Skeel condition number (68) of the factor R . This example demonstrates that straightforward numerical orthogonalization cannot effectively counteract the effects of finite precision, resulting in approximations that behave similarly as regularized approximations.

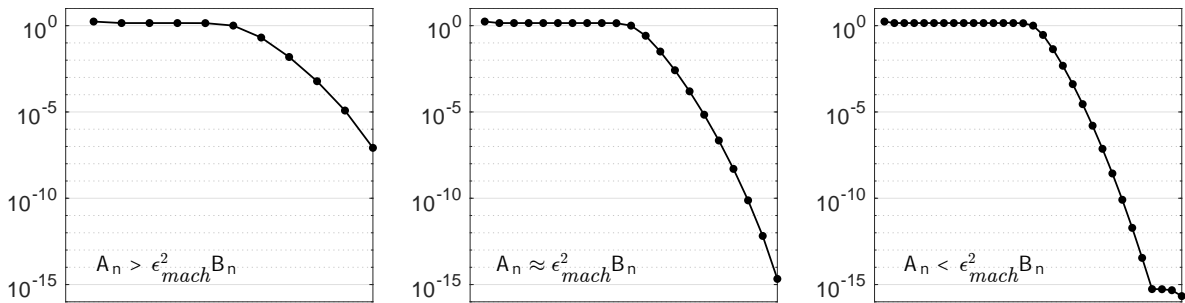


Figure 9: Singular value profile of the synthesis operator associated with $\Phi_n = \{\text{Re}(\exp(ik\pi x/2))\}_{k=0}^n$ for $n = 10$ (left), $n = 20$ (middle), and $n = 30$ (right), computed in double precision using Chebfun [24]. Analytically, the singular values decrease exponentially toward zero as n goes to infinity. The singular values are linked to the frame bounds A_n and B_n of Φ_n via (19). The spanning set is numerically redundant starting from $n = 20$, i.e., when $A_n \approx \epsilon_{mach}^2 B_n$.

Hence, for all $\mathbf{x} \in \mathbb{C}^{n'}$ it holds that

$$\begin{aligned} \|f - \mathcal{T}_n \widehat{\mathbf{c}}\|_H &\leq \|(f + \widehat{\Delta}f) - (\mathcal{T}_n + \widehat{\Delta}\mathcal{T}_n)\widehat{\mathbf{c}}\|_H + \|\widehat{\Delta}f\|_H + \|\widehat{\Delta}\mathcal{T}_n \widehat{\mathbf{c}}\|_H, \\ &\leq \|(f + \widehat{\Delta}f) - (\mathcal{T}_n + \widehat{\Delta}\mathcal{T}_n)\mathbf{x}\|_H + \|\widehat{\Delta}f\|_H + \|\widehat{\Delta}\mathcal{T}_n \widehat{\mathbf{c}}\|_H, \\ &\leq \|f - \mathcal{T}_n \mathbf{x}\|_H + 2\|\widehat{\Delta}f\|_H + \|\widehat{\Delta}\mathcal{T}_n \widehat{\mathbf{c}}\|_H + \|\widehat{\Delta}\mathcal{T}_n \mathbf{x}\|_H. \end{aligned}$$

The final bound follows from $\|\widehat{\Delta}\mathcal{T}_n\|_{2,H} \leq C \epsilon_{\text{mach}} \|\mathcal{T}_n\|_{2,H}$ and $\|\widehat{\Delta}f\|_H \leq C \epsilon_{\text{mach}} \|f\|_H$.

For the second result, note that

$$\|\widehat{\mathbf{c}}\|_2 = \|(\mathcal{T}_n + \widehat{\Delta}\mathcal{T}_n)^\dagger (f + \widehat{\Delta}f)\|_2 \leq \frac{\|f + \widehat{\Delta}f\|_H}{\sigma_{\min}(\mathcal{T}_n + \widehat{\Delta}\mathcal{T}_n)},$$

where σ_{\min} denotes the smallest singular value. Using (19), we obtain $\sigma_{\min}(\mathcal{T}_n + \widehat{\Delta}\mathcal{T}_n) \geq \sigma_{\min}(\mathcal{T}_n) - \|\widehat{\Delta}\mathcal{T}_n\|_{2,H} = \sqrt{A_n} - C \epsilon_{\text{mach}} \sqrt{B_n} > 0$, such that

$$\|\widehat{\mathbf{c}}\|_2 \leq \frac{\|f + \widehat{\Delta}f\|_H}{\sqrt{A_n} - C \epsilon_{\text{mach}} \sqrt{B_n}}.$$

Furthermore, we have that $\mathcal{P}_n f \in V_n$ and, hence, there exist coefficients $\mathbf{c} \in \mathbb{C}^{n'}$ such that $\mathcal{P}_n f = \mathcal{T}_n \mathbf{c}$ with $\|\mathbf{c}\|_2 \leq \|\mathcal{P}_n f\|_H / \sqrt{A_n}$ (20). The final result follows from choosing $\mathbf{x} = \mathbf{c}$, i.e.,

$$\begin{aligned} \|f - \mathcal{T}_n \widehat{\mathbf{c}}\|_H &\leq \|f - \mathcal{T}_n \mathbf{c}\|_H + C \epsilon_{\text{mach}} \left(\sqrt{B_n} (\|\widehat{\mathbf{c}}\|_2 + \|\mathbf{c}\|_2) + 2\|f\|_H \right) \\ &\leq \|f - \mathcal{P}_n f\|_H + C \epsilon_{\text{mach}} \left(\sqrt{B_n} \left(\frac{\|f + \widehat{\Delta}f\|_H}{\sqrt{A_n} - C \epsilon_{\text{mach}} \sqrt{B_n}} + \frac{\|\mathcal{P}_n f\|_H}{\sqrt{A_n}} \right) + 2\|f\|_H \right) \\ &\leq \|f - \mathcal{P}_n f\|_H + C \epsilon_{\text{mach}} \left(\frac{(1 + C \epsilon_{\text{mach}})\sqrt{B_n}}{\sqrt{A_n} - C \epsilon_{\text{mach}} \sqrt{B_n}} + \sqrt{\frac{B_n}{A_n}} + 2 \right) \|f\|_H. \end{aligned}$$

□

Proof of Theorem 6. For any linear operator $\Delta\mathcal{T}_n$ mapping from $\mathbb{C}^{n'}$ to H and any $\Delta f \in H$, we have that

$$\|f - \mathcal{T}_n \widehat{\mathbf{c}}\|_H \leq \|(f + \Delta f) - (\mathcal{T}_n + \Delta\mathcal{T}_n)\widehat{\mathbf{c}}\|_H + \|\Delta f\|_H + \|\Delta\mathcal{T}_n \widehat{\mathbf{c}}\|_H.$$

Since $\widehat{\mathbf{c}}$ is computed by a backward stable algorithm with stability constant C , there exist $\widehat{\Delta}\mathcal{T}_n$ and $\widehat{\Delta}f$ satisfying $\|\widehat{\Delta}\mathcal{T}_n\|_{2,H} \leq C \epsilon_{\text{mach}} \|\mathcal{T}_n\|_{2,H}$ and $\|\widehat{\Delta}f\|_H \leq C \epsilon_{\text{mach}} \|f\|_H$ such that

$$\widehat{\mathbf{c}} = \arg \min_{\mathbf{x} \in \mathbb{C}^{i_n}} \|(f + \widehat{\Delta}f) - (\mathcal{T}_n + \widehat{\Delta}\mathcal{T}_n)\mathbf{x}\|_H^2 + \epsilon^2 \|\mathbf{x}\|_2^2.$$

Therefore, for all $\mathbf{x} \in \mathbb{C}^{n'}$,

$$\begin{aligned} \|(f + \widehat{\Delta}f) - (\mathcal{T}_n + \widehat{\Delta}\mathcal{T}_n)\widehat{\mathbf{c}}\|_H^2 + \epsilon^2 \|\widehat{\mathbf{c}}\|_2^2 &\leq \|(f + \widehat{\Delta}f) - (\mathcal{T}_n + \widehat{\Delta}\mathcal{T}_n)\mathbf{x}\|_H^2 + \epsilon^2 \|\mathbf{x}\|_2^2 \\ \Rightarrow \|(f + \widehat{\Delta}f) - (\mathcal{T}_n + \widehat{\Delta}\mathcal{T}_n)\widehat{\mathbf{c}}\|_H + \epsilon \|\widehat{\mathbf{c}}\|_2 &\leq \sqrt{2} \left(\|(f + \widehat{\Delta}f) - (\mathcal{T}_n + \widehat{\Delta}\mathcal{T}_n)\mathbf{x}\|_H + \epsilon \|\mathbf{x}\|_2 \right). \end{aligned}$$

Hence, it holds that

$$\begin{aligned} \|f - \mathcal{T}_n \widehat{\mathbf{c}}\|_H &\leq \|(f + \widehat{\Delta}f) - (\mathcal{T}_n + \widehat{\Delta}\mathcal{T}_n)\widehat{\mathbf{c}}\|_H + \|\widehat{\Delta}f\|_H + \|\widehat{\Delta}\mathcal{T}_n \widehat{\mathbf{c}}\|_H, \\ &\leq \|(f + \widehat{\Delta}f) - (\mathcal{T}_n + \widehat{\Delta}\mathcal{T}_n)\widehat{\mathbf{c}}\|_H + C \epsilon_{\text{mach}} \|f\|_H + \epsilon \|\widehat{\mathbf{c}}\|_2, \\ &\leq \sqrt{2} \left(\|(f + \widehat{\Delta}f) - (\mathcal{T}_n + \widehat{\Delta}\mathcal{T}_n)\mathbf{x}\|_H + \epsilon \|\mathbf{x}\|_2 \right) + C \epsilon_{\text{mach}} \|f\|_H, \\ &\leq \sqrt{2} \|f - \mathcal{T}_n \mathbf{x}\|_H + (1 + \sqrt{2})\epsilon \|\mathbf{x}\|_2 + (1 + \sqrt{2})C \epsilon_{\text{mach}} \|f\|_H, \end{aligned}$$

where in the second step it was used that $\epsilon \geq C \epsilon_{\text{mach}} \|\mathcal{T}_n\|_{2,H}$. □

B Proof of Theorem 10

For completeness, we first prove an equivalent characterization of (44).

Lemma 3. For any $\epsilon > 0$,

$$k_n^\epsilon(\mathbf{x}) = z(\mathbf{x})(G_n + \epsilon^2 I)^{-1} z(\mathbf{x})^*,$$

where $z(\mathbf{x}) = [\phi_1(\mathbf{x}) \ \dots \ \phi_{n'}(\mathbf{x})] \in \mathbb{C}^{1 \times n'}$ and G_n represents $\mathcal{T}_n^* \mathcal{T}_n$.

Proof. G_n is positive semidefinite such that there exists an eigenvalue decomposition of the form $V \Sigma^2 V^*$, where $V \in \mathbb{C}^{n' \times n'}$ is unitary and $\Sigma \in \mathbb{C}^{n' \times n'}$ is diagonal. Moreover, this implies that the synthesis operator \mathcal{T}_n associated with Φ_n has a singular value decomposition of the form $\sum_{i=1}^n \sigma_i u_i \mathbf{v}_i^*$ where $\{u_i\}_{i=1}^n$ is an orthonormal basis for V_n , \mathbf{v}_i are the first n columns of V and $\sigma_i = (\Sigma)_{i,i}$ for $i = 1 \dots n$. Therefore, using $z(\mathbf{x}) = \sum_{i=1}^n \sigma_i u_i(\mathbf{x}) \mathbf{v}_i^*$, we obtain

$$\begin{aligned} z(\mathbf{x})(G_n + \epsilon^2 I)^{-1} z(\mathbf{x})^* &= \left(\sum_{i=1}^n \sigma_i u_i(\mathbf{x}) \mathbf{v}_i^* \right) V (\Sigma^2 + \epsilon^2 I)^{-1} V^* \left(\sum_{i=1}^n \sigma_i \overline{u_i(\mathbf{x})} \mathbf{v}_i \right) \\ &= \left(\sum_{i=1}^n \sigma_i u_i(\mathbf{x}) \mathbf{v}_i^* V \right) (\Sigma^2 + \epsilon^2 I)^{-1} \left(\sum_{i=1}^n \sigma_i \overline{u_i(\mathbf{x})} V^* \mathbf{v}_i \right) \\ &= [\sigma_1 u_1(\mathbf{x}) \ \dots \ \sigma_n u_n(\mathbf{x})] (\Sigma^2 + \epsilon^2 I)^{-1} [\sigma_1 \overline{u_1(\mathbf{x})} \ \dots \ \sigma_n \overline{u_n(\mathbf{x})}]^\top \\ &= \sum_{i=1}^n \frac{\sigma_i^2}{\sigma_i^2 + \epsilon^2} |u_i(\mathbf{x})|^2, \end{aligned}$$

which equals (44). □

We are now ready to prove Theorem 10.

Proof of Theorem 10. Note that

$$\frac{1}{2}(G_n + \epsilon^2 I) \preceq G_{n,m} + \epsilon^2 I \preceq \frac{3}{2}(G_n + \epsilon^2 I) \quad \Rightarrow \quad (31) \text{ with } A_{n,m}^\epsilon = \frac{1}{2}.$$

The inequality on the left is exactly the Δ -spectral approximation introduced in [10, eq. (2)] with $\Delta = 1/2$. This allows us to reuse the method of proof of [10, Lemma 6]. Analogously, using the eigenvalue decomposition of $G_n + \epsilon^2 I = V \Sigma^2 V^*$ we find that it suffices to show that

$$\|\Sigma^{-1} V^* G_{n,m} V \Sigma^{-1} - \Sigma^{-1} V^* G_n V \Sigma^{-1}\|_2 \leq 1/2$$

holds with probability $1 - \gamma$. Define a rank-one random matrix

$$X(\mathbf{x}) = w(\mathbf{x}) \Sigma^{-1} V^* z(\mathbf{x})^* z(\mathbf{x}) V \Sigma^{-1},$$

where \mathbf{x} is distributed according to μ and where $z(\mathbf{x})$ is defined as in Lemma 3. Then, $\Sigma^{-1} V^* G_{n,m} V \Sigma^{-1}$ is equal to the sum of m i.i.d. copies of this random matrix, i.e.,

$$\Sigma^{-1} V^* G_{n,m} V \Sigma^{-1} = \frac{1}{m} \sum_{j=1}^m X_j.$$

Since $\mathbb{E}(X_j) = \Sigma^{-1} V^* G_n V \Sigma^{-1}$, we can use the matrix concentration result [10, Lemma 27]. Using Lemma 3, we bound

$$\|X_j\|_2 = w(\mathbf{x}_j) z(\mathbf{x}_j) (G_n + \epsilon^2 I)^{-1} z(\mathbf{x}_j)^* = w(\mathbf{x}_j) k_n^\epsilon(\mathbf{x}_j) \leq K_{w,n}^\epsilon,$$

and

$$\mathbb{E}(X_j^2) = \mathbb{E}(w(\mathbf{x}_j) k_n^\epsilon(\mathbf{x}_j) X_j) \preceq K_{w,n}^\epsilon \Sigma^{-1} V^* G_n V \Sigma^{-1} = K_{w,n}^\epsilon (I - \epsilon^2 \Sigma^{-2}),$$

where $K_{w,n}^\epsilon := \max_{\mathbf{x} \in X} (w(\mathbf{x}) k_n^\epsilon(\mathbf{x}))$ and $I \in \mathbb{R}^{n \times n}$ is the identity matrix. Defining

$$E := K_{w,n}^\epsilon (I - \epsilon^2 \Sigma^{-2}) = K_{w,n}^\epsilon \text{diag}(\sigma_1^2 / (\sigma_1^2 + \epsilon^2), \dots, \sigma_n^2 / (\sigma_n^2 + \epsilon^2)),$$

where σ_i is the i -th singular value of \mathcal{T}_n , this results in

$$\begin{aligned} \Pr \left(\left\| \frac{1}{m} \sum_{j=1}^m X_j - \Sigma^{-1} V^* G_n V \Sigma^{-1} \right\|_2 \geq 1/2 \right) &\leq \frac{8 \operatorname{Tr}(E)}{\|E\|_2} \exp \left(\frac{-m/8}{\|E\|_2 + K_{w,n}^\epsilon/3} \right) \\ &\leq 16n^\epsilon \exp \left(\frac{-3}{32} \frac{m}{K_{w,n}^\epsilon} \right) \leq \gamma \end{aligned}$$

where in the second step we used the assumption $\sigma_1^2 = \|G\|_2 \geq \epsilon^2$. \square

C Asymptotics of DPSWFs

In this section, we aim to motivate that the maxima $\|u_i\|_{L^\infty[-W,W]}$ associated to the one-dimensional Fourier extension frame (60) are $\mathcal{O}(\sqrt{n})$ as $n \rightarrow \infty$. In order to do so, observe that

$$\|u_i\|_{L^\infty[-W,W]} = \|U_{i-1}(n, W)\|_{L^\infty[-W,W]} / \sqrt{\lambda_{i-1}(n, W)}, \quad (70)$$

where $U_k(n, W)$ and $\lambda_k(n, W)$ are the discrete prolate spheroidal wave functions (DPSWFs) and the associated eigenvalues analysed by Slepian in [46]. We recall and examine their asymptotic behaviour for the different regimes identified in [46, section 2.4-2.5]. Numerical evidence confirms that (70) is bounded by $\mathcal{O}(\sqrt{n})$, as is the case for the prolate spheroidal wave functions [14, Prop. 3.1], the continuous analogues of the DPSWFs.

Given the asymptotic expansions outlined in [46, section 2.4-2.5], we can derive that as $n \rightarrow \infty$:

- for $i \leq 2nW + 1$,

$$\|u_i\|_{L^\infty[-W,W]} = \mathcal{O}(\sqrt{n}), \quad (71)$$

- for $i = \lfloor 2nW + (b/\pi) \log(n) \rfloor + 1$ with fixed $b > 0$,

$$\|u_i\|_{L^\infty[-W,W]} \sim r(E\beta) \sqrt{\beta} \exp(\pi E\beta/4) \sqrt{\frac{3\pi(1 + \exp(\pi b))}{\beta(1 + \exp(\pi E\beta)) \ln(n)}} \sqrt{n}, \quad (72)$$

where r , E and β are defined by [46, eq. (52)-(54)],

- for $i = \lfloor 2nW(1 + \epsilon) \rfloor + 1$ with fixed $0 < \epsilon < 1/2W - 1$,

$$\|u_i\|_{L^\infty[-W,W]} \sim L_2^{-1/2} \pi(1 - \cos(2\pi W))^2)^{-1/4} \sqrt{n}, \quad (73)$$

where L_2 is defined by [46, eq. (47)] with $A = -\cos(2\pi W)$ and $k = n - (i - 1)$,

- for $i = n - l$ with fixed $0 \leq l$,

$$\|u_i\|_{L^\infty[-W,W]} \sim \sqrt{\pi} \left(\frac{2}{1 - \cos(2\pi W)} \right)^{1/4} \sqrt{n}. \quad (74)$$

The result for $i \leq 2nW + 1$ follows from considering

$$\begin{aligned} \|u_i\|_{L^\infty[-W,W]} &\leq \|u_i\|_{L^\infty[-1/2,1/2]} \\ &= \|U_{i-1}(n, W)\|_{L^\infty[-1/2,1/2]} / \sqrt{\lambda_{i-1}(n, W)} \\ &\leq \sqrt{n} / \sqrt{\lambda_{i-1}(n, W)}, \end{aligned}$$

where we used the Nikolskii inequality [41, Theorem 1] with $\|U_{i-1}(n, W)\|_{L^2[-1/2,1/2]} = 1$. Furthermore,

$$1/\sqrt{\lambda_{i-1}(n, W)} \leq 1/\sqrt{\lambda_{\lfloor 2nW \rfloor}(n, W)} \sim \sqrt{2}$$

using [46, eq. (60)]. Hence, we get $\|u_i\|_{L^\infty[-W,W]} = \mathcal{O}(\sqrt{n})$, where the proportionality factor is at most approximately $\sqrt{2}$.

For the case of $i \geq 2nW + 1$, it follows from [43, Corollary 2] and the fact that the DPSWFs are even or odd that

$$\|u_i\|_{L^\infty[-W,W]} = \frac{\|U_{i-1}(n, W)\|_{L^\infty[-W,W]}}{\sqrt{\lambda_{i-1}(n, W)}} = \frac{|U_{i-1}(n, W; \omega = 2\pi W)|}{\sqrt{\lambda_{i-1}(n, W)}}.$$

Hence, the maximum is achieved at the boundary. Furthermore, by combining [46, eq. (50) and (60)] for $U_k(n, W)$ and $\lambda_k(n, W)$ for $k = i - 1 = \lfloor 2nW + (b/\pi) \log(n) \rfloor$ with fixed b , one obtains

$$\frac{|U_k(n, W; \omega = 2\pi W)|}{\sqrt{\lambda_k(n, W)}} \sim r(E\beta) \sqrt{\beta} \exp(\pi E\beta/4) \sqrt{\frac{3\pi(1 + \exp(\pi b))}{\beta(1 + \exp(\pi E\beta)) \ln(n)}} \sqrt{n}$$

Similarly, for $k = i - 1 = \lfloor 2nW(1 + \epsilon) \rfloor$ with fixed $0 < \epsilon < 1/2W - 1$ we derive from [46, eq. (42), (56), (57) and (63)] that

$$\frac{|U_k(n, W; \omega = 2\pi W)|}{\sqrt{\lambda_k(n, W)}} \sim L_2^{-1/2} \pi (1 - \cos(2\pi W)^2)^{-1/4} \sqrt{n},$$

while for $k = i - 1 = n - l$ with fixed $l \geq 1$ we derive from [46, eq. (13), (38) and (58)] that

$$\frac{|U_k(n, W; \omega = 2\pi W)|}{\sqrt{\lambda_k(n, W)}} \sim \sqrt{\pi} \left(\frac{2}{1 - \cos(2\pi W)} \right)^{1/4} \sqrt{n}.$$

Acknowledgements

We greatly appreciate the fruitful discussions and helpful suggestions provided by Ben Adcock, Felix Bartel, Nick Dewaele, Karlheinz Gröchenig, Christopher Musco, Thijs Steel, Alex Townsend, Nick Trefethen, and Raf Vandebril.

Funding

The first author is a Ph.D fellow of the Research Foundation Flanders (FWO), funded by grant 11P2T24N.

References

- [1] B. Adcock. Optimal sampling for least-squares approximation. *arXiv preprint arXiv:2409.02342*, 2024.
- [2] B. Adcock, S. Brugiapaglia, and C. G. Webster. *Sparse Polynomial Approximation of High-Dimensional Functions*. SIAM, Philadelphia, PA, 2022.
- [3] B. Adcock and A. C. Hansen. A generalized sampling theorem for stable reconstructions in arbitrary bases. *J. Fourier Anal. Appl.*, 18:685–716, 2012.
- [4] B. Adcock, A. C. Hansen, and C. Poon. Beyond consistent reconstructions: Optimality and sharp bounds for generalized sampling, and application to the uniform resampling problem. *SIAM J. Math. Anal.*, 45(5):3132–3167, 2013.
- [5] B. Adcock and D. Huybrechs. Frames and numerical approximation. *SIAM Rev.*, 61(3):443–473, 2019.
- [6] B. Adcock and D. Huybrechs. Frames and numerical approximation II: Generalized sampling. *J. Fourier Anal. Appl.*, 26(6):87, 2020.
- [7] B. Adcock, D. Huybrechs, and J. Martín-Vaquero. On the numerical stability of Fourier extensions. *Found. Comput. Math.*, 14(4):635–687, 2014.

- [8] B. Adcock and A. Shadrin. Fast and stable approximation of analytic functions from equispaced samples via polynomial frames. *Constr. Approx.*, 57(2):257–294, 2023.
- [9] A. Alaoui and M. W. Mahoney. Fast randomized kernel ridge regression with statistical guarantees. *Adv. Neural Inf. Process. Syst.*, 28:775–783, 2015.
- [10] H. Avron, M. Kapralov, C. Musco, C. Musco, A. Velingker, and A. Zandieh. Random Fourier features for kernel ridge regression: Approximation bounds and statistical guarantees. In *Int. Conf. Mach. Learn. ICML*, pages 253–262. PMLR, 2017.
- [11] H. Avron, M. Kapralov, C. Musco, C. Musco, A. Velingker, and A. Zandieh. A universal sampling method for reconstructing signals with simple Fourier transforms. In *Proc. 51st Annu. ACM SIGACT Symp. Theory Comput.*, STOC 2019, pages 1051–1063. Association for Computing Machinery, 2019.
- [12] P. Berger, K. Gröchenig, and G. Matz. Sampling and reconstruction in distinct subspaces using oblique projections. *J. Fourier Anal. Appl.*, 25(3):1080–1112, 2019.
- [13] R. Bhatia. *Notes on Functional Analysis*. Hindustan Book Agency, New Delhi, 2009.
- [14] A. Bonami, G. Kerkycharian, and P. Petrushev. Gaussian bounds for the heat kernel associated to prolate spheroidal wave functions with applications. *Constr. Approx.*, 57(2):351–403, 2023.
- [15] J. P. Boyd. *Chebyshev and Fourier Spectral Methods*. Dover Publications, Mineola, NY, 2nd edition, 2001.
- [16] P. D. Brubeck, Y. Nakatsukasa, and L. N. Trefethen. Vandermonde with Arnoldi. *SIAM Rev.*, 63(2):405–415, 2021.
- [17] O. Christensen et al. *An Introduction to Frames and Riesz Bases*. Birkhäuser, Basel, 2003.
- [18] A. Cohen, M. A. Davenport, and D. Leviatan. On the stability and accuracy of least squares approximations. *Found. Comput. Math.*, 13:819–834, 2013.
- [19] A. Cohen and G. Migliorati. Optimal weighted least-squares methods. *SMAI J. Comput. Math.*, 3:181–203, 2017.
- [20] V. Coppé, D. Huybrechs, R. Matthysen, and M. Webb. The AZ algorithm for least squares systems with a known incomplete generalized inverse. *SIAM J. Matrix Anal. Appl.*, 41(3):1237–1259, 2020.
- [21] I. Daubechies. *Ten Lectures on Wavelets*. SIAM, Philadelphia, PA, 1992.
- [22] E. B. Davies and M. Plum. Spectral pollution. *IMA J. Numer. Anal.*, 24(3):417–438, 2004.
- [23] M. Dolbeault and A. Cohen. Optimal sampling and Christoffel functions on general domains. *Constr. Approx.*, 56(1):121–163, 2022.
- [24] T. A. Driscoll, N. Hale, and L. N. Trefethen. *Chebfun Guide*. Pafnuty Publications, Oxford, 2014.
- [25] Z. Drmac. On principal angles between subspaces of euclidean space. *SIAM J. Matrix Anal. Appl.*, 22(1):173–194, 2000.
- [26] T. Erdélyi. Markov–Nikolskii type inequalities for exponential sums on finite intervals. *Adv. Math.*, 208(1):135–146, 2007.
- [27] W. Gautschi. *Orthogonal Polynomials: Computation and Approximation*. Oxford University Press, Oxford, 2004.
- [28] G. Golub. *Rosetak Document 4: Rank Degeneracies and Least Square Problems*. NBER Working Paper Series No. W0165. National Bureau of Economic Research, Cambridge, Mass, 1977.
- [29] K. Gröchenig. Sampling, Marcinkiewicz–Zygmund inequalities, approximation, and quadrature rules. *J. Approx. Theory*, 257:105455, 2020.

- [30] A. Herremans and D. Huybrechs. Efficient function approximation in enriched approximation spaces. *IMA J. Numer. Anal.*, page drae017, 2024.
- [31] A. Herremans and D. Huybrechs. SamplingWithNumericalRedundancy. <https://github.com/aherremans/SamplingWithNumericalRedundancy>, 2025.
- [32] A. Herremans, D. Huybrechs, and L. N. Trefethen. Resolution of singularities by rational functions. *SIAM J. Numer. Anal.*, 61(6):2580–2600, 2023.
- [33] N. J. Higham. The accuracy of solutions to triangular systems. *SIAM J. Numer. Anal.*, 26(5):1252–1265, 1989.
- [34] N. J. Higham. *Accuracy and Stability of Numerical Algorithms*. SIAM, Philadelphia, PA, 2nd edition, 2002.
- [35] D. Huybrechs. On the Fourier extension of nonperiodic functions. *SIAM J. Numer. Anal.*, 47(6):4326–4355, 2010.
- [36] S. Karnik, J. Romberg, and M. A. Davenport. Improved bounds for the eigenvalues of prolate spheroidal wave functions and discrete prolate spheroidal sequences. *Appl. Comput. Harmon. Anal.*, 55:97–128, 2021.
- [37] H. J. Landau and H. O. Pollak. Prolate spheroidal wave functions, Fourier analysis and uncertainty—III: The dimension of the space of essentially time- and band-limited signals. *Bell Syst. Tech. J.*, 41(4):1295–1336, 1962.
- [38] R. Matthysen and D. Huybrechs. Function approximation on arbitrary domains using Fourier extension frames. *SIAM J. Numer. Anal.*, 56(3):1360–1385, 2018.
- [39] R. A. Meyer, C. Musco, C. Musco, D. P. Woodruff, and S. Zhou. Near-linear sample complexity for L_p polynomial regression. In *Proc. 2023 Annu. ACM-SIAM Symp. Discrete Algorithms SODA*, pages 3959–4025. SIAM, 2023.
- [40] G. Migliorati. Multivariate approximation of functions on irregular domains by weighted least-squares methods. *IMA J. Numer. Anal.*, 41(2):1293–1317, 2021.
- [41] R. J. Nessel and G. Wilmes. Nikolskii-type inequalities for trigonometric polynomials and entire functions of exponential type. *J. Aust. Math. Soc.*, 25(1):7–18, 1978.
- [42] P. Nevai. Géza Freud, orthogonal polynomials and Christoffel functions. A case study. *J. Approx. Theory*, 48(1):3–167, 1986.
- [43] K. A. Said and A. A. Beex. Non-asymptotic bounds for discrete prolate spheroidal wave functions analogous with prolate spheroidal wave function bounds. *Appl. Comput. Harmon. Anal.*, 63:20–47, 2023.
- [44] P. F. Shustin and H. Avron. Semi-infinite linear regression and its applications. *SIAM J. Matrix Anal. Appl.*, 43(1):479–511, 2022.
- [45] R. D. Skeel. Scaling for numerical stability in Gaussian elimination. *J. ACM*, 26(3):494–526, 1979.
- [46] D. Slepian. Prolate spheroidal wave functions, Fourier analysis, and uncertainty—V: The discrete case. *Bell Syst. Tech. J.*, 57(5):1371–1430, 1978.
- [47] G. W. Stewart. *Matrix Algorithms: Volume 1: Basic Decompositions*. SIAM, Philadelphia, PA, 1988.
- [48] N. Stylianopoulos. An Arnoldi Gram-Schmidt process and Hessenberg matrices for orthonormal polynomials. Slides from talk at Banff International Research Station, 2010.